Active Control of Passive Safety in Passenger Motor Vehicles

A feasibility study investigating dynamic denting of members using pyrotechnic devices

Prepared by: N.S. Marshall
Department of Mechanical Engineering
University of Cape Town
in partial completion of a Masters Degree in Mechanical Engineering.

Prepared for : Prof. G.N. Nurick
Department of Mechanical Engineering
University of Cape Town

(September 1995)

Acknowledgements

I would like to express my sincere thanks to the following people without whom this thesis would have been impossible:

Prof. Gerald Nurick, for his patience and invaluable encouragement,

Mr J. Larsson and the Volvo Car Corporation for motivation and financial support,

The Foundation for Research and Development for financial support,

Mr L. Watkins, Mr. A. Warburton, Mr H. Thomlinson, Mr M. Jolivet, and Mr W. Slaverse for guidance in the workshop and for making the jigs and specimens,

Mr J. Fitton, for all his computer assistance,

The S.A.B.S for use of their testing facilities.

Synopsis

This report describes a feasibility study investigating dynamic denting of members using pyrotechnic devices to engineer favourable energy absorption characteristics into thin walled tubes. A tube of sufficiently low slenderness ratio and wall thickness, when loaded axially to failure, will collapse in the progressive buckling mode. After the ultimate buckling load has been exceeded, and as the tube continues to compress, the load oscillates between loads considerably lower than the ultimate buckling load. The object of introducing an advantageous deformation is to decrease the ultimate buckling load to a magnitude comparable with the subsequent peak loads, but at the same time avoiding a change in the buckling mode which is not advantageous.

Testing was limited to thin walled square mild steel tubes. The test procedure began with a process to determine the limitations imposed on the geometric imperfections that could be achieved by the use of explosive. It was found that all the explosively induced deformations were rounded, i.e. the dents were hemi-spherical in shape. It was also found that a smooth edged round hole could be created in the centre of the dent with the use of a round, flat explosive charge.

Geometric imperfections that could be induced explosively in the specimens (as well as other deformation shapes, tested for comparative purposes) were mechanically formed in the specimens. The tubes were then quasi - statically crushed to determine the energy absorption characteristics induced by the deformations. When spherical dents were induced, the deformation affected the tube beyond the immediate spherical dent and hence the distance between the plastic hinges was increased and instabilities in the crushing process were introduced. Holes (without any visible denting) decreased the distance between the plastic hinges and thus also induced instabilities. In both cases the tubes tended to skew over to one side and in extreme cases Euler buckling ensued.

The next stage of the experiments included testing of tubes deformed with spherical dents and centrally positioned holes. The combination of the two appeared to be compensatory. The ultimate buckling load was decreased and the distance between the plastic hinges could

be adjusted by a combination of the dent depth and the hole diameter, i.e. an optimum combination could result in the distance between the plastic hinges being equal to the natural wavelength of the tube.

Finally, flat, circular explosive charges were used to induce a combination of dents with centrally positioned holes in 100mm square mild steel tubes with a wall thickness of 2mm. Different combinations of dent depth and hole diameter were compared. For these tube dimensions it was found that a corner dent depth of between 7 and 10 mm, with a hole of diameter 50mm (half the tube width) was optimum. The ultimate buckling load was decreased significantly and symmetric progressive buckling occurred.

TABLE OF CONTENTS

List of Illustrations

List of Tables

Nomenclature

δ	effective crushing distance
ε	strain
$\dot{\varepsilon}$	strain rate
ϕ	diameter
l	distance between plastic hinges
σ	stress
σ_o	static flow stress
σ'_o	dynamic flow stress
σ_y	yield stress
μ	poisson's ratio
A	area
C	width of square tube
Cd	centre depth of deformation
Cl	centre length of deformation
D	Cowper-Symonds constant
E	Young's modulus
Ed	depth of deformation at the corners of the tube
El	length of deformation at the corners of the tube
F	force
H	wall thickness
M_o	fully plastic moment
P_{mean} or P_m	mean static collapse load
P_m^d	mean dynamic collapse load
P_{ult}	ultimate buckling load
R	tube radius
b_e	effective support width
b_f	final radius of toroidal surface
h	height of the explosive charge
l	length of the explosive charge
m	mass of the explosive charge
q	Cowper-Symonds constant
t	wall thickness
v	velocity
w	width of the explosive charge

Original (undeformed) tube Tube with no visible geometric imperfections

Deformed tube	Tube with visible geometric imperfections induced either mechanically or explosively
Crushed tube	Tube that has been axially loaded in compression until failure
Natural wavelength	The total distance between three plastic hinges

1. INTRODUCTION

Thin walled structures have been used extensively in energy absorbing applications, particularly in the petro-chemical and nuclear industries as well as in motor vehicles for energy absorption during a collision[1]. The buckling mode of thin walled tubes can be engineered to absorb large amounts of excess energy in a cost efficient way. In this context many studies have been done in the past in order to characterise[2-7] and in some cases change or tailor[8-12] the buckling characteristics of thin walled tubes. This project deals specifically with the influence of pyrotechnically induced deformations on the buckling characteristics of thin walled square tubes.

Two problems may be encountered with the use of thin walled tubes as energy absorbers. Firstly, the ultimate buckling load (or initial peak force in the load displacement curve of an axially compressed tube, refer to figure 2.2) can be of the order of twice the magnitude of subsequent peaks. The very high first peak results in a very much greater deceleration than the deceleration associated with the buckling of the remainder of the tube. In some situations the maximum deceleration is limited by, for example, human survival limits during a motor vehicle accident[13]. At the same time the energy absorbed by a unit length of the energy absorbing component is determined by the average magnitude of the load, and thus subsequent peak forces should not be reduced. Ideally the magnitude of all peaks should be the same[13].

The second problem is the tendency for a tube to skew over to one side (thus inducing the Euler Buckling mode) if it is not loaded perfectly axially.[8] The Euler buckling mode results in a significant decrease in the effective stroke of the energy absorption component, and consequently a lower total energy absorption. The use of pyrotechnically induced deformations prior to

collapse of the tube has been proposed as a means of overcoming both problems. This project is a feasibility study of the proposal.

The project was divided into three sections. First, tests were performed in order to determine the limitations imposed on the deformations that could be induced in thin walled square tubes with the use of plastic explosive charges. The second part involved mechanical simulation of the deformation shapes. The deformed tubes were then crushed quasi-statically in order to determine the effects of the deformations on the buckling characteristics of the thin walled square tubes. Finally, those deformation shapes that proved to have beneficial effects on the buckling characteristics of the tubes, in terms of energy absorption were reproduced explosively. The explosively deformed tubes were crushed quasi-statically in order to confirm the results.

The report begins with a literature survey that includes the following: Background into the different modes of compressive failure of thin walled tubes and the implications of the different modes on the energy absorption capacity of the tubes; the development of analytical predictions of mean crushing load for the different failure modes; discussion of the ultimate buckling load (or first peak force) of thin walled tubes; and previous studies on different geometric deformations induced in tubes in order to decrease the ultimate buckling load and / or to ensure the more effective modes of buckling for energy absorption.

Chapter three contains a description of the experimental techniques used, while the results are presented in tabulated and graphical form in chapter four. Discussion of the results and the implications to energy absorption are presented in chapter five, and chapter six is a summary of the conclusions thereof.

2. LITERATURE REVIEW

2.1 Modes of Buckling

Thin walled column structures loaded axially may fail in a combination of one or more of three distinct collapse modes: Euler buckling, Progressive buckling, and Plastic buckling. These modes are discussed briefly in terms of energy absorption characteristics during collapse and final collapse shape.

2.1.1 Euler Buckling

The tube bends in a manner similar to a strut. A plastic mechanism develops locally in the tube and the tube 'folds over" such that the longitudinal axes on either side of the hinge are no longer parallel. A typical load displacement curve of a specimen which has failed in this manner is shown in figure 2.1 [14] below. The total length of the tube was approximately 380mm. The length of the deflection during which significant energy absorption occurs is very short relative to the total length of the tube.

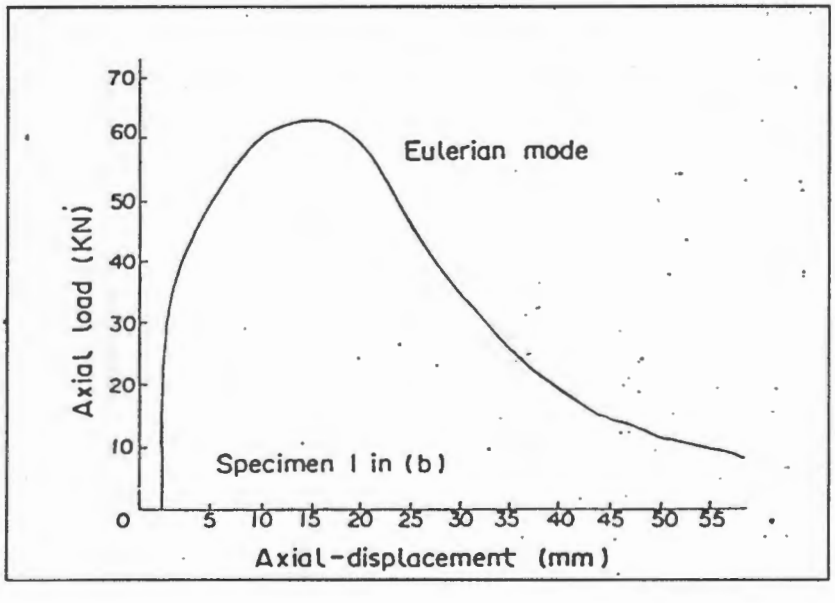

Fig. 2.1 Load-displacement curve for the Euler buckling mode of a typical thin walled tube [14]

The Euler mode of buckling was found to occur in cylindrical [14] and square [15] tubes with large length to width ratios as seen in figures 2.3 and 2.4. Jones and Abramowicz [4] also found that imperfections in the asymmetric progressive buckling modes tended to cause the tube to exhibit overall bending.

Since the energy absorption occurs in a small local position relative to the total length of the structure, the effective stroke is very short, the Euler Buckling mode is not efficient for energy absorption. Euler buckling should therefore be avoided in energy absorbers constructed from thin walled tubes.

2.1.2 Progressive Buckling

When an axial compressive load is applied to a structure which exceeds the ultimate strength of the structure, the load carrying capacity of the structure usually decreases significantly. In the case of progressive buckling of thin walled tubes, the load increases again after reaching a minimum load and begins to oscillate about a mean load. These oscillations correspond to the formation of concertina type lobes. A typical load-deflection curve for the progressive buckling phenomenon of a thin walled square tube is shown in figure 2.2.

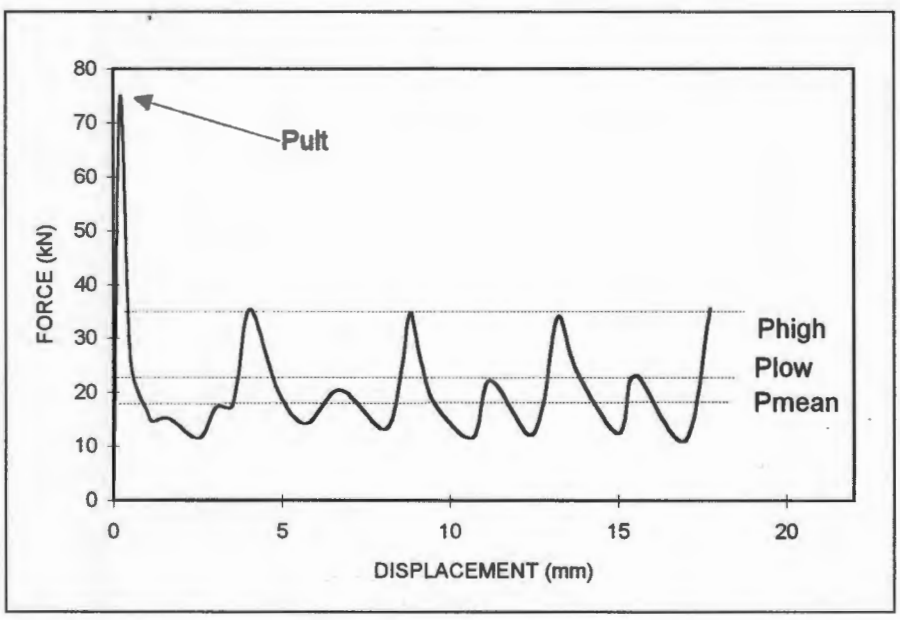

Fig. 2.2 Load-Displacement Curve of Progressive Buckling of a thin walled square tube.

The first peak corresponds with the formation of plastic hinges in the structure. The walls of the tube fold around and extend at the hinges. One layer of folds occurs at a time and once the first layer is completely formed the next layer begins. Folding usually begins at one end and then extends progressively to the other end, hence the name progressive buckling. Each layer of lobes is associated with a pair of peaks on the load displacement curve shown in figure 2.2. The physical crumpling is described extensively in the literature by Jones [13] among others.

There is significant energy absorbed by the collapse of the tube even after the deflection of the tube associated with the initial collapse load (the first peak force). It is this property that makes the progressive buckling of thin walled tubular structures suitable for energy absorption purposes.

2.1.2.1 Different Modes of Progressive Buckling

The term progressive buckling refers to a number of different geometric folding patterns. These different folding patterns all have similarly oscillating load-displacement characteristics, but slightly different mean crushing loads.

2.1.2.1.1 Thin Walled Cylindrical Tubes

Progressive buckling of thin walled cylinders results in either axisymmetric (concertina type), or non-axisymmetric (diamond) modes of collapse[5].

i Concertina mode - Three plastic hinges form around the circumference of the tube and the tube folds to form ring shaped bulges down the length of the tube.

ii Diamond mode - In this failure mode the tube crumples progressively by forming a number of diamond shapes around the circumference which then fold in half over each other [2]. The number of diamonds that form around the circumference varies.

Andrews *et al* [14] showed the effect of the original geometric parameters of cylindrical aluminium tubes on their collapse mode, see figure 2.3.

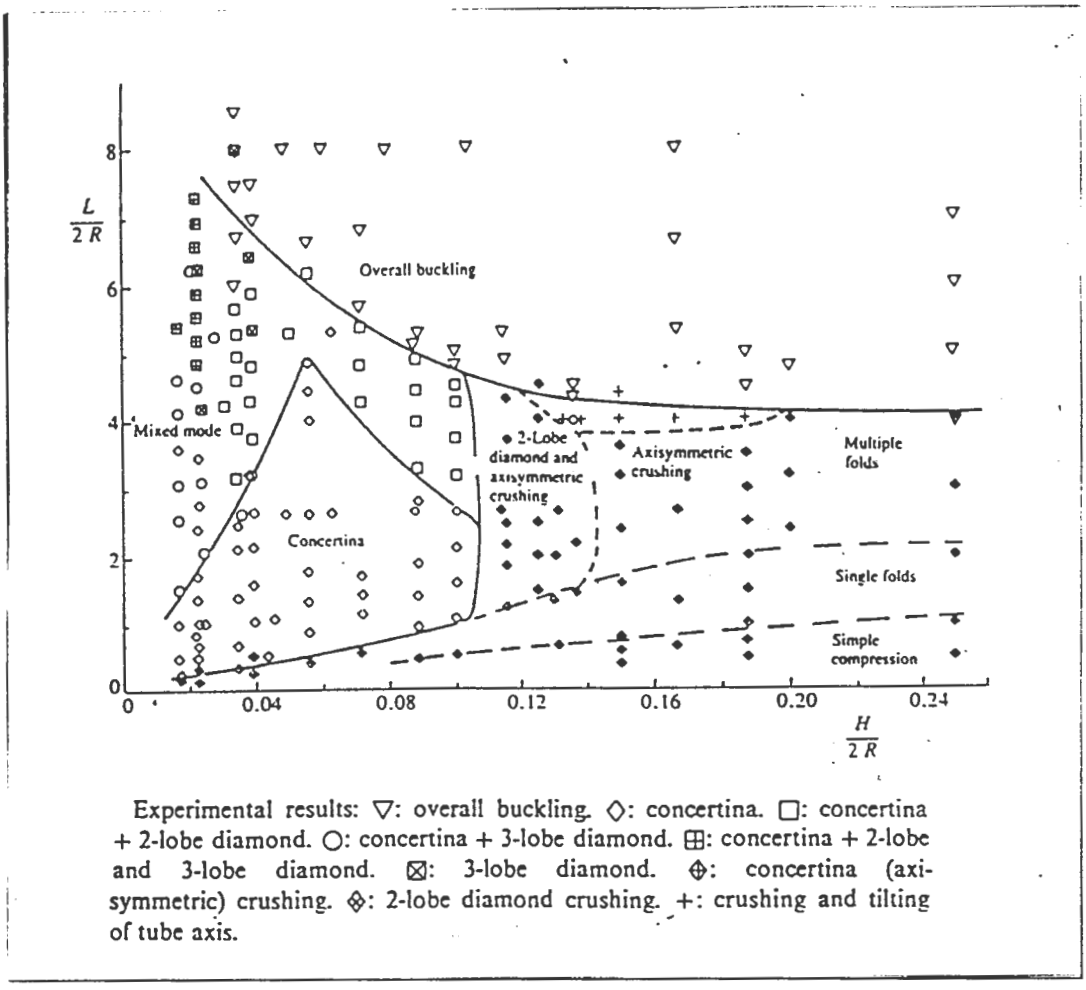

Experimental results: ▽: overall buckling. ◇: concertina. □: concertina + 2-lobe diamond. ○: concertina + 3-lobe diamond. ⊞: concertina + 2-lobe and 3-lobe diamond. ⊠: 3-lobe diamond. ⊕: concertina (axi-symmetric) crushing. ⊗: 2-lobe diamond crushing. +: crushing and tilting of tube axis.

Fig. 2.3 Classification chart for collapse modes of cylindrical aluminium alloy tubes[14]

2.1.2.1.2 Thin Walled Square Tubes

There are four distinct progressive buckling modes of failure for square tubes loaded axially as identified by Abramowicz and Jones [4] :

i Symmetric modes - describes three geometric folding mechanisms all with identical crushing loads and energy absorption characteristics:

a) two opposite lobes in one layer move outwards while the other two move inwards.

b) all four lobes move inwards

c) Three lobes move inwards while one moves outwards.

ii Asymmetric mixed mode "type A" - describes crushing consisting of a combination of symmetric layers (as described previously) and layers of lobes that form with three lobes moving outwards and one lobe moving inwards.

iii Asymmetric mixed mode "type B" - describes a combination of symmetric layers and layers with two adjacent lobes moving inwards and the other two outward.

iv Extensional mode - all four lobes move outwards.

Korneck [15] studied the effect of the original tube dimensions on the collapse mode of axially crushed square tubes. The results show the effect of the slenderness ratio (length / width) and the ratio of wall thickness / width. The trends are displayed in figure 2.4.

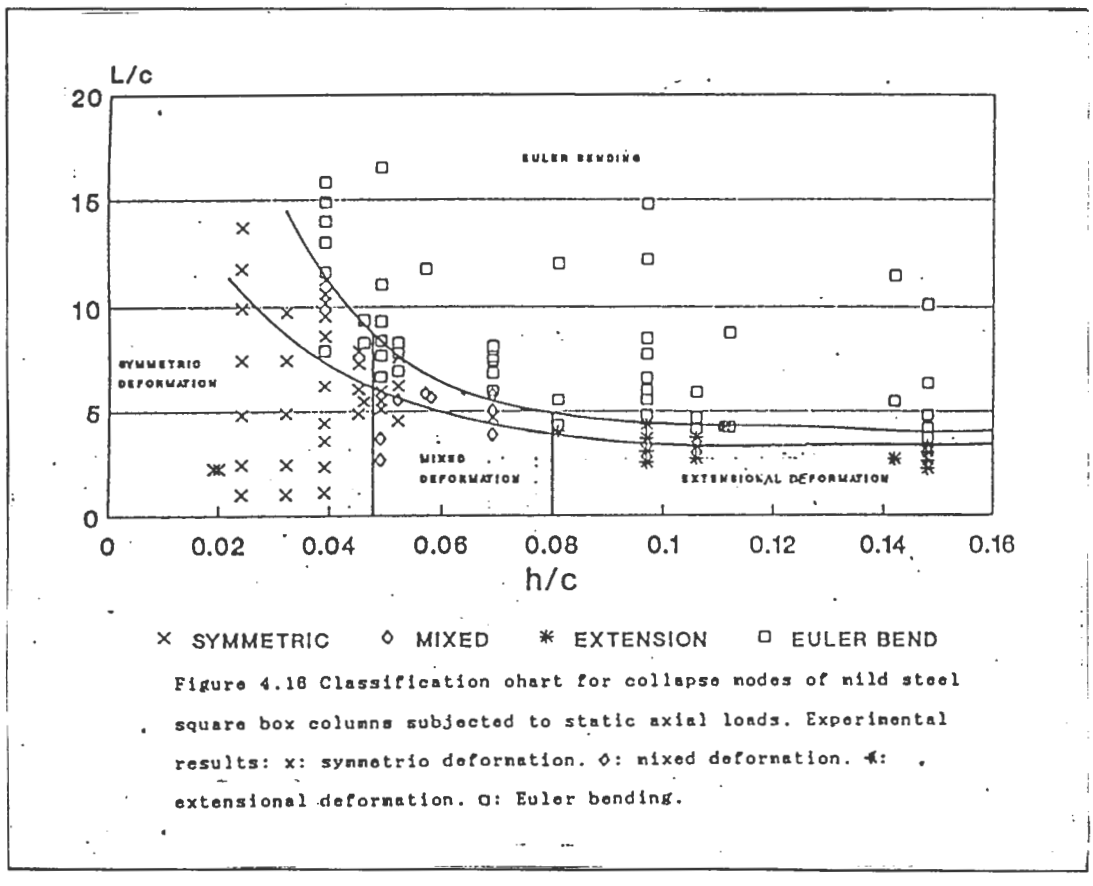

Fig. 2.4 Classification chart for collapse modes of mild steel square tubes [15]

The results show that very long tubes tended to fail by Euler Buckling, and an increase in the wall thickness also induced Euler Buckling. The mode of progressive buckling appears to be significantly determined by the wall thickness of the tube.

2.1.3 Dynamic Plastic Buckling

In most situations for which thin walled tubular structures are used as energy absorbers, a large amount of energy must be dissipated rapidly. The tube clearly does not fail quasi-statically. If Euler buckling is avoided, the tube may crumple either by dynamic progressive buckling, as discussed in section 2.1.2, or by dynamic plastic buckling. In the former case, both lateral and axial inertia effects are neglected, while in the later case inertia effects play a large role. The type of buckling is therefore determined by the duration of the impact load and the magnitude of the striking mass.

The typical shape of a tube crushed in the dynamic plastic buckling mode is described by Jones [13] and usually consists of wavelike 'ripples' along the length of the tube. Unlike progressive buckling the lobes are not squashed flat on top of one another.

For dynamic progressive buckling the load duration is much longer than the transit time of an elastic stress wave travelling the distance of the tube. The mass of the striking object is large by comparison to the mass of the crumpling tube. It is evident from experimental data that the structural effectiveness (the ratio of mean crushing load to the load to cause uniform plastic flow) is usually less than unity [13]. The structural effectiveness may exceed unity in cases where the flow stress is increased by strain hardening or strain rate effects.

In order for dynamic plastic buckling to occur the load duration is comparable to the transit time of an elastic stress wave travelling the distance of the tube and thus the inertia effects are considerable. The mass of the striking object may be similar to the mass of the crumpling tube for dynamic plastic buckling to occur. It

was determined that the structural effectiveness must be greater than unity for dynamic plastic buckling in a cylindrical tube struck by a mass [13].

Dynamic plastic buckling is of great importance in the aerospace, nuclear and petrochemical industries where the impact velocities are very great. In the field of structural crashworthiness of motor vehicles, dynamic progressive buckling is more prevalent, as the impact velocities are relatively much smaller. The example in Appendix I illustrates this point.

Since the results and objectives of this project are aimed at applications of motor vehicle accidents, the project is restricted to the study of progressive buckling.

2.2 Mean Static Buckling Load

The mean buckling load is important from an energy absorption aspect. The mean buckling load is used to approximate the total energy that would be absorbed by a tube if the whole length of the tube was completely crushed. Initially empirical relations were developed for use as design tools [2, 6]. Later more rigorous analyses were done to predict actual mean loads [4-7, 17-21]. In cases where very complex shaped tubes are used, Finite Element Analysis has been found to be a very useful tool[22, 23].

Traditionally, in analytical predictions of mean crushing load it has been assumed that one lobe forms completely before any buckling begins in the next lobe [4-6, 17, 18] More recently this assumption has been modified by Wierzbicki *et al* [7] to consist of a double folding wave being the active crumpling zone at any instant. The mean force was then calculated by equating the external work done by a mean force acting over the crushing distance to the internal energy dissipation by plastic bending and extension.

2.2.1 Static Progressive Buckling of Circular Tubes.

The analytical prediction of the mean crushing load, shown by P_{mean} in figure 2.2 of cylindrical tubes has been studied extensively [5, 6, 21] since Pugsley and Macaulay [2], and Alexander [3] pioneered the work in 1960.

2.2.1.1 Non-axisymmetric (diamond) Deformation Mode

The analysis proposed by Pugsley and Macaulay [2] was based on the non-axisymmetric or diamond deformation mode of circular tubes. In this failure mode the tube crumples progressively by forming a number of diamond shapes around the circumference which then fold in half over each other. Pugsley and Macaulay [2] first studied the actual geometry of the crushed lobes and based their analysis on the physical crumpling process. The external work done was equated to the internal work done in crushing the tube. The external work was approximated by the average crushing force over a distance corresponding to complete flattening of one fold. The energy absorbed in the plastic bending along the lines of the final folds, and the deformation of the material between the fold lines approximates the internal work done. Hence the mean load (P_{mean}) was given by:

$$\frac{P_{mean}}{P_0} = \left(C_1 \frac{t}{R} + C_2 \right) \qquad \text{...eqn 1}$$

where $C_1 = 1.6$ and $C_2 = 0.36\nu$ for $n = 3$

and

$C_1 = 2.1$ and $C_2 = 0.45\nu$ for $n = 4$

where ν is Poisson's Ratio, n is the number of lobes around the circumference of the tube, $P_0 = 2\pi RH\sigma$ is the load to cause yield in simple compression and C1 and C2 were determined empirically.

Pugsley [24] later amended this equation taking into account strain hardening effects. Wierzbicki is cited by Abramowicz and Jones [5] as having derived an approximate expression for the mean crushing force, which is expressed as

$$\frac{P_m}{M_o} = 62.88\left(\frac{2R}{H}\right)^{\frac{1}{3}} \qquad \text{...eqn 2}$$

where M_o is the fully plastic moment given by :

$$M_o = \frac{2\sigma_o}{\sqrt{3}}\frac{H^2}{4} \qquad \text{...eqn 3}$$

2.2.1.2 Axisymmetric (concertina) Deformation Mode

Alexander [3] considered the axisymmetric or concertina deformation mode. Internal work done is split into the energy absorbed by two stationary plastic hinges, one plastic hinge moving laterally and the stretching of the material between the plastic hinges.

Alexander assumed that:

- each lobe was flattened completely
- lobes did not start to deform until the previous lobe was completely flattened
- the mean circumferential strain was constant throughout the material between the hinges, i.e. the variation in the strain with axial position was neglected.

The analysis was done first for lobes forming outside the tube diameter and then repeated for lobes forming inside the tube diameter. The final solution was an average of the two.

This was an approximate analysis but gave fair correlation with experiments and was used as the basis for later work reported by Johnson *et al* [21], Jones [13], Abramowicz and Jones [5, 6], and Wierzbicki and Bhat [25] . Wierzbicki *et al* [7] found that the mean collapse load for the complete collapse of one load was underestimated by as much as 40%, as shown in figure 2.5[7].

Abramowicz [26] recognised that the tube did not fold flat and found an expression for the mean crushing distance. Abramowicz and Jones [5, 6] improved on Alexander's solution for axisymmetric crushing of circular tubes discussed above with the introduction of the mean crushing distance and Wierzbicki and Bhat [25] replaced the stationary hinges with moving ones.

Wierzbicki *et al* [7] introduced an active crush zone consisting of two folding waves instead of one. This has led to a model that realistically predicts the load displacement curve of a collapsing tube, with finite maxima and minima and alternating high and low peaks. The predicted mean crushing force gave very close results to experimentally measured values if the flow stress was taken as 92% of the ultimate tensile strength of the material as shown in figure 2.5.

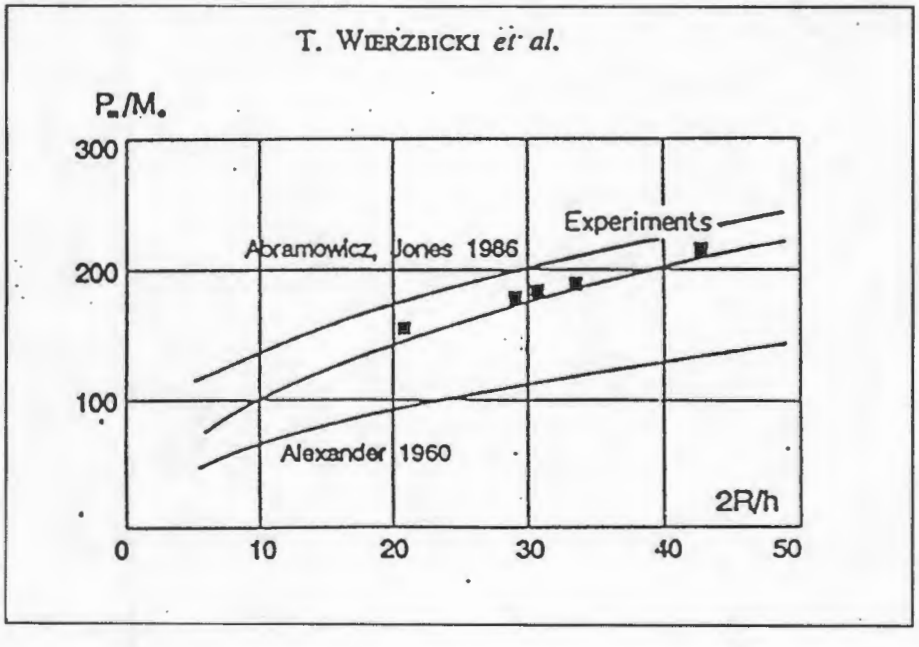

Fig. 2.5 Comparison of experimentally measured mean crushing force with prediction of various theories [7].

2.2.2 Static Progressive Buckling of Square Tubes

The theoretical analysis of the progressive buckling of square tubes uses a rigorous kinematic approach suitably generalised for large displacements. Two basic collapse elements were developed by Wierzbicki and Abramowicz [18], and Hayduk and Wierzbicki [27], type I and type II, shown in figure 2.6. The type II element was modified by Abramowicz and Jones [6]. From these two elements the four possible collapse modes, described in section 2.1.2.1, can be constructed [4]. The internal energy dissipation associated with the elements includes two thirds by bending contributions at the plastic hinges, and the rest by extension of the shell in small localised positions [4, 18]. This is therefore an improvement on the initial inextensional predictions made by Wierzbicki and Akerstrom [19] and Ohkubo *et al* [20], as one third of the energy dissipation is attributed to the extension. The two basic collapse elements were developed for plate intersections of 90°. They were later modified and extended to include intersections of any angle [28]. The modifications include the use of two elements in series, first a quasi-inextensional element and then, as the crushing process proceeds, an extensional element. This change only affects the mean crushing force by between four and eight percent. The main difference is that more of the energy absorbed is attributed to extensional deformation.

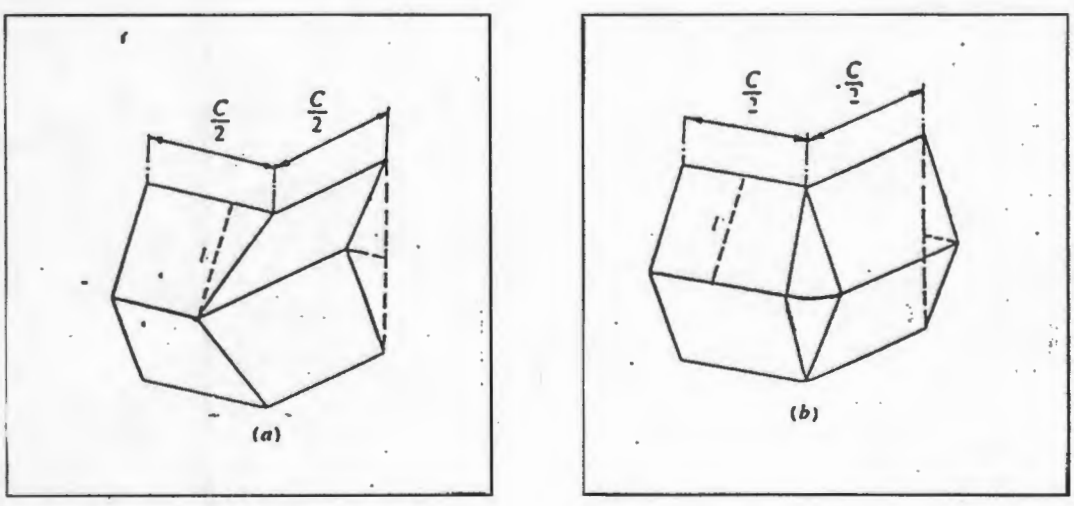

Fig. 2.6. Basic collapse elements (a) Type I and (b) Type II [13]

The internal energy dissipation in all the elements required to construct the collapse mode is equated to the external energy dissipated as the crushing force moves through a certain distance. The effective crushing distance found by Abramowicz [26] is used to predict the distance over which crushing will occur.

Abramowicz and Jones [4] found the mean crushing load by minimising the energy equation with respect to the distance between the plastic hinges and the radius of the extensional surface. Abramowicz and Jones [6] developed the following expressions for the mean static crushing load using the improved type II element:

i Symmetric mode

$$\frac{P_m}{M_o} = 52.22\left(\frac{C}{H}\right)^{\frac{1}{3}} \qquad \textit{...eqn 4a}$$

and

$$\frac{l}{H} = 0.99\left(\frac{C}{H}\right)^{\frac{2}{3}} \qquad \textit{...eqn 4b}$$

Using Wierzbicki and Abramowicz's [28] method the coefficients in equation 4a changed slightly to give:

$$\frac{P_m}{M_o} = 48.46\left(\frac{C}{H}\right)^{0.37} \qquad \textit{...eqn 4c}$$

ii Asymmetric mixed mode 'type A"

$$\frac{P_m}{M_o} = 42.92\left(\frac{C}{H}\right)^{\frac{1}{3}} + 3.17\left(\frac{C}{H}\right)^{\frac{2}{3}} + 2.04 \qquad \textit{...eqn 5a}$$

and

$$\frac{l}{H} = 0.78\left(\frac{C}{H}\right)^{\frac{2}{3}} \qquad \textit{...eqn 5b}$$

iii Asymmetric mixed mode 'type B"

$$\frac{P_m}{M_o} = 45.90\left(\frac{C}{H}\right)^{\frac{1}{3}} + 1.75\left(\frac{C}{H}\right)^{\frac{2}{3}} + 1.02 \qquad \text{...eqn 6a}$$

and $$\frac{l}{H} = 0.86\left(\frac{C}{H}\right)^{\frac{2}{3}} \qquad \text{...eqn 6b}$$

iv Extensional mode

$$\frac{P_m}{M_o} = 32.64\left(\frac{C}{H}\right)^{\frac{1}{2}} + 8.16 \qquad \text{...eqn 7a}$$

and $$\frac{l}{H} = \left(\frac{C}{H}\right)^{\frac{1}{2}} \qquad \text{...eqn 7b}$$

2.3 Mean Dynamic Buckling Load (material strain rate sensitivity)

The plastic flow in some materials is dependent on the rate of strain of the material. This is known as 'strain rate sensitivity". Mild steel is known to display a high degree of strain rate sensitivity and van Kuren and Scott [29] found that the energy absorbed by a thin walled tube increased as the velocity of deformation increased. Cowper and Symonds cited in [13] suggested a constitutive equation relating the dynamic flow stress to the strain rate and the static flow stress as follows:

$$\frac{\sigma'_o}{\sigma_o} = 1 + \left(\frac{\dot{\varepsilon}}{D}\right)^{1/q} \qquad \text{...eqn 8a}$$

where traditionally q = 5 and D = 40.4 s^{-1} for mild steel, although a certain amount of uncertainty about these coefficients exists because of the scarcity of data from which to determine them. The coefficients used by Abramowicz and Jones [4, 5, 6] are D = 6844 s^{-1} and q = 3.91 or D = 802 s^{-1} and q = 3.585. (The graphs in figures 2.7a and 2.7b, taken from reference [4], illustrate the effect of these coefficients.)

Since $\sigma = \frac{F}{A}$, and area is assumed to be constant, the mean dynamic crushing load can be related to the static crushing load by:

$$\frac{P_m^d}{P_m} = 1 + \left(\frac{\dot{\varepsilon}}{D}\right)^{1/q} \qquad \text{...eqn 8b}$$

There is a certain amount of difficulty in predicting the strain rate due to the complex crushing mechanism. Expressions are derived for an estimate of the strain rate by Abramowicz and Jones for square tubes [4] and for circular tubes [5].

For square tubes collapsing in the symmetric mode the following expressions were derived [4]:

$$\dot{\varepsilon} = \frac{Hv_m}{2b_f\delta} \qquad \text{...eqn 9a}$$

where: mean velocity $v_m = v/2$ ...eqn 9b

final rolling radius $\frac{b_f}{l} = 0.53\left(\frac{C}{H}\right)^{\frac{1}{3}}$ ...eqn 9c

and hence

$$\frac{P_m^d}{M_o} = 52.22\left\{1 + \left(\frac{0.33v}{CD}\right)^{\frac{1}{q}}\right\}\left(\frac{C}{H}\right)^{\frac{1}{3}} \qquad \text{...eqn 10}$$

Figures 2.7a and 2.7b show the predicted mean dynamic load on 1.5"(38.1mm) square tube with a wall thickness of 0.045"(1.2mm) and 2"(50.8mm) square tubes with a wall thickness of 0.065"(1.6mm) respectively. The data points are from Abramowicz and Jones [6].

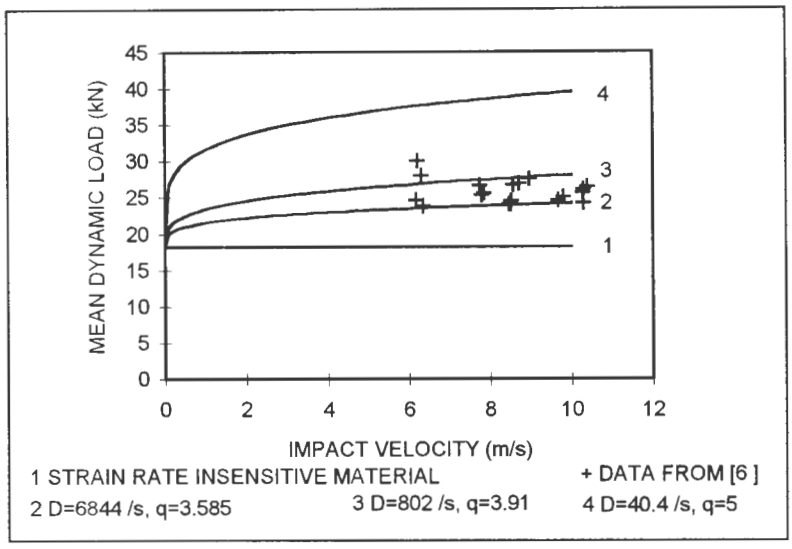

Fig. 2.7a Strain rate effect predictions for 1.5"(38mm) mild steel tubing [6]

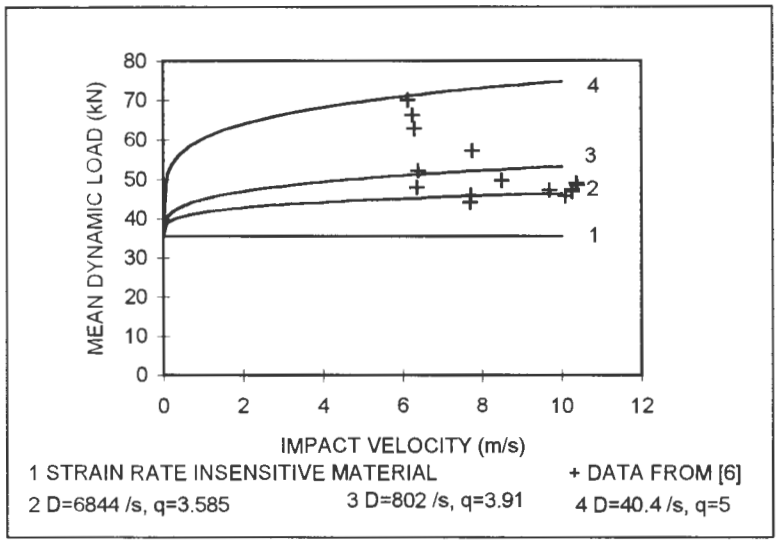

Fig. 2.7b Strain rate effect predictions for 2"(50.8mm) mild steel tubing [6]

The equations for the crumpling of cylindrical tubes and square tubes failing by other collapse modes can be found in references [5, 6]. The equations have not been repeated here as this report is restricted to the study of symmetric collapse of square tubes.

The crushing geometry of axially loaded thin walled tubes does not appear to be affected significantly by the rate of crushing [13]. It was for this reason that quasi-static testing was considered to be acceptable for the purposes of this project.

2.4 Ultimate Buckling Load

The ultimate buckling load for tubes failing by progressive buckling may be far greater than the subsequent peak loads as was illustrated in figure 2.2. The ultimate load is governed by elastic-plastic buckling. Classically the ultimate buckling load can be approximated by:

$$P_{ult} = \sigma_o A \qquad \text{...eqn 11}$$

Where σ_o is the plastic flow stress and A is the cross sectional area of the tube.

Wierzbicki and Abramowicz [28] found that the flow stress could be approximated by 92% of the ultimate tensile stress

Meng *et al* [17] used von Karman's postulate that simplifies elastic plastic behaviour of thin plates loaded axially in compression by assuming that the entire load is supported by two strips of equal width at either side of the plate. The middle portion is assumed to carry negligible load. The ultimate buckling load is then found when the load carrying part of the plate extends the whole way across the plate. The flow stress, σ_o in equation (11) can then be approximated by:

$$\sigma_o = \frac{2\alpha\sigma_y t}{C} \qquad \text{...eqn 12a}$$

with

$$\alpha^2 = \frac{\pi^2 E}{12(1-\mu^2)\sigma_y} \qquad \text{...eqn 12b}$$

The above equations gave fair agreement with experiments carried out by Meng *et al* [17], however the experiments showed an exponential increase in critical stress while the equation predicts a linear increase as the ratio of the wall thickness to characteristic width of the tube ($^t/_C$) increases.

Mamalis *et al* [30, 31] and Belingardi *et al* [32, 33] found that as ($^{t}/_{c}$) increased, so the difference between the initial peak load and the subsequent peak loads decreased for circular tubes. This indicates that the initial peak load would not need to be decreased as much for thicker tubes in order to give more uniform load-displacement characteristics.

In order to avoid Euler type buckling the ultimate buckling load must be lower than the critical Euler bucking load. Basic theory of Euler buckling of struts [34, 35] shows that the critical Euler buckling load decreases with an increase in slenderness ratio. This is consistent with the tests done by Korneck [15] on square mild steel tubes and Andrews *et al* [14] on circular aluminium tubes. (See figures 2.4 and 2.3 respectively.)

2.5 Geometric Imperfections

There are two reasons for introducing geometric imperfections into a thin walled tube being used as an energy absorption component:

a) to decrease the initial peak force, and
b) to force a particular buckling mode on the crushing column.

An ideal energy absorber for most situations causes a uniform deceleration during the entire stroke. The ideal structure should thus deform at a constant force throughout its collapse. As has already been discussed, a thin walled tube collapses with a very high initial peak force. The force then oscillates between lower forces as the tube continues to crumple. If the peak force can be reduced to the same magnitude as the subsequent peaks, a more ideal energy absorber would exist.

It is accepted that the introduction of geometric imperfections affects the initial peak force [8-12, 32, 36-38]. Langseth *et al* [36] used a prebuckle imposed by applying a

preload to the tube quasi - statically. It was found that the magnitude of the initial peak force decreased with an increase in the amplitude of the prebuckle.

In many real situations a force may not be applied exactly axially to the tube. The tube is then likely to buckle in the Euler buckling mode. It has been found that denting of the tubular structure tends to force the buckling mode to follow the shape of the imperfection [8, 9]. This can be used to force progressive buckling to occur.

2.5.1 Sharp Corner Dents

Schriever and Helling [8] conducted a series of tests on square box columns with sharp dents on the corners at different distances apart. The dents were characterised by their depth and the included angle. Figure 2.8 schematically illustrates the geometry of the dents tested by Schriever and Helling [8].

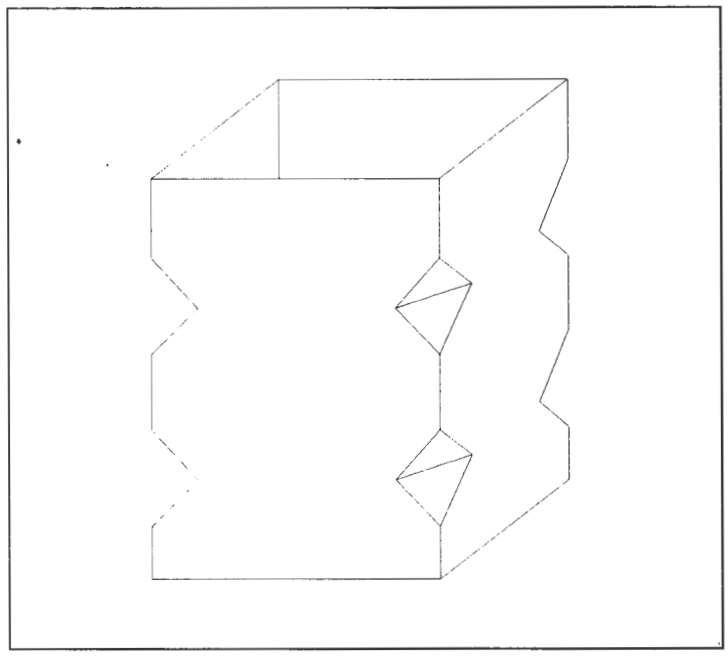

Fig 2.8 Imperfections in the tube corners as used by Schriever and Helling [8]

It was found that for imperfections positioned at a distance equal to the natural half wavelength apart, the peak force decreased by 17%. The mean crushing

load also decreased by 10% but since the geometric efficiency increased by 7% the total energy absorption over the entire stroke was comparable to an undented structure. If the imperfections were positioned closer together the regularity of deformation was lost and thus so was the stability of the collapse mode.

It was found that while undented specimens tended towards the Euler buckling mode when the force was applied at an angle of up to 5.5° to the longitudinal axis of the tube, dented specimens still followed the progressive buckling mode.

2.5.2 Sharp Side Dents

Korneck [15] performed a series of tests on mild steel square tubes to determine the effect of side dents on the crumpling characteristics of the tubes. A 90° angled denter was used to form the dents. An idealisation of the dents is shown in figure 2.9. As anticipated it was found that the ultimate buckling load was decreased by predenting the structure.

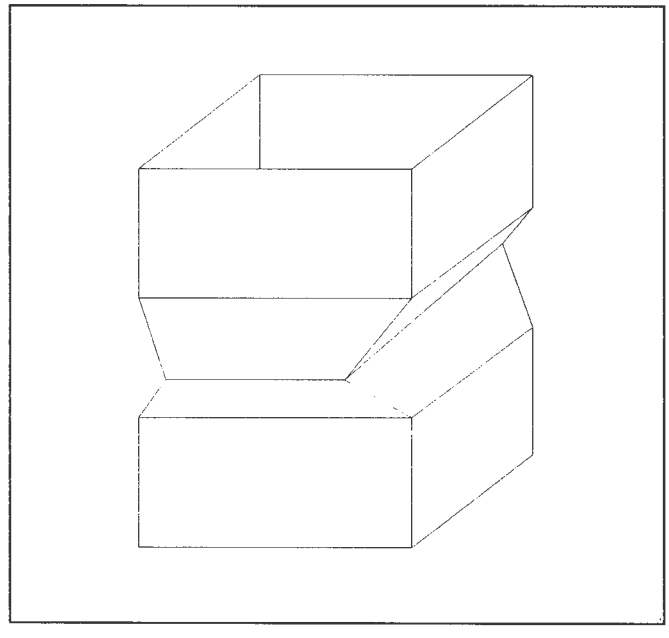

Fig 2.9 The idealised geometry of sharp side pre dents in square tubes [15]

The pre-dent did not appear to change the other buckling characteristics significantly. It was found that the buckling mode stabilised into the normal progressive buckling mode by the formation of the third peak force. It was assumed that the third peak force could be used as the average magnitude of the high peak load. The optimum dent depth could therefore be approximated by finding the depth of predent that resulted in an ultimate load equal in magnitude to the third peak load. Figure 2.10 shows this relationship for 50mm square mild steel tubes with a wall thickness of 1.2mm .

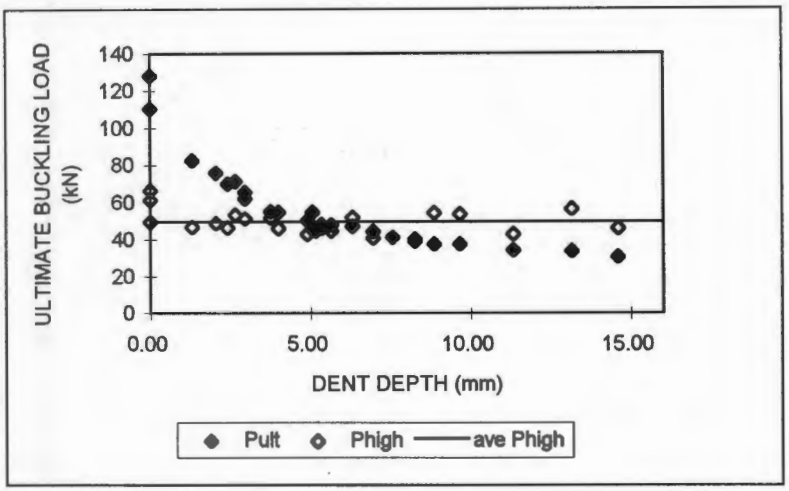

Fig 2.10 Optimum dent depth for 50x50x1.2mm mild steel tubes [15]. Pult and Phigh are defined in figure 2.2.

The mean buckling load was found to remain unchanged by the predent. The mean load was found for the formation of three lobes by the area under the load displacement curve.

Dynamic tests on similarly prepared specimens showed that the folding geometry remained unchanged by increased strain rates. The mean collapse load was found to increase as would be expected for a strain rate sensitive material like mild steel. The dynamic tests were conducted using a drop hammer with a maximum trolley mass of 58.6 kg and a maximum height of 4.5m.

2.5.3 Circular Cut-outs

It seems reasonable to approximate a rectangular section tube by four flat plates [9, 17, 39]. Analytical and experimental analysis on the stability of thin plates with a centrally positioned circular hole have been done extensively. As has already been discussed, the von Karman principle is used to simplify the elastic - plastic analysis. A thin plate subjected to uniaxial compressive loading, with the longitudinal edges pinned but not loaded experiences plastic yield starting at the longitudinal edges. The von Karrman effective width was described by Surko [9] as:

$$b_e = 1.9t\sqrt{\frac{E}{\sigma_y}} \qquad \text{...eqn 13}$$

which means that if the diameter of the hole is smaller than

$$\phi \leq C - 1.9t\sqrt{\frac{E}{\sigma_y}} \qquad \text{...eqn 14}$$

then the hole should have little or no effect on the buckling characteristics of the plate.

Numerous experimental studies have been reported [10 - 12] on the effect of cut-outs on the peak load of axially compressed cylinders. The ultimate buckling load was found to be governed by the parameter $\alpha = \frac{a}{\sqrt{Rt}}$ where a is the characteristic cut-out dimension, R is the cylinder radius and t is the wall thickness. For $\alpha \leq 1.0$, the cut-out had no appreciable effect. For values of $1.0 < \alpha < 2.0$ there was a sharp decrease in ultimate load with an increase in α. For $\alpha > 2.0$ there was a small decrease in the ultimate load with an increase in α [10]. The tests carried out by Toda [10] were performed on polyester cylinders.

Tests on aluminium and mild steel tubes of different diameters and wall thickness were carried out by Gupta *et al* [12]. Holes of different diameters and configurations were drilled in the tubes. It was found that the ultimate buckling load was decreased. The collapse was initiated at the position of the holes. In the

case of long tubes which would normally buckle in the Euler mode, [14]. progressive buckling occurred. This is probably because the ultimate buckling load was lowered to below the Euler critical load.

The mean buckling load was not greatly affected by the presence of holes.

A numerical analysis reported by Kormi *et al* [11] on thin circular tubes with one large side opening shows qualitative agreement with experiments. The circumferential dimension of the opening had a large effect on the ultimate buckling load. The longitudinal dimension had little effect on the ultimate load but did change the progressive buckling mode.

2.5.4 Combined Structural Deformations

Surko [9] performed a limited experimental study of the effect of combined structural imperfections on the ultimate buckling load and the collapse mode of box columns. Seven tests were conducted on box columns manufactured from 140mm square plates with a wall thickness of 1.6mm welded together. Two stiffened plates were welded to the ends of the columns to produce a clamped boundary condition. The imperfections were introduced before the plates were welded together.

The range of tests included specimens with two different deformation shapes, two centrally positioned circular holes of different diameters, and edge crack patterns, as well as a test on an undeformed specimen for comparative purposes.

The two deflection shapes considered were a pyramidal bulge from the corners of the side plates outwards to the centre, with no deflection at the edges, and an outward accordion shaped bulge which resembled the extensional collapse mode. The diameters of the holes compared were 41% and 61% of the width of the tube (57.4mm and 85.4mm respectively).

The undented specimen buckled in the symmetrical mode, while the buckling shape of the dented specimens was dictated by the dent shape. The dents lowered the peak load considerably, and the effect of deformed corners was greatest. The mean crushing load was not significantly changed although this aspect was not completely covered as the box columns were crushed to between 14% and 50% of their original length, which was approximately one wavelength. Small holes had little effect on the peak force and the decrease in peak load was small with large increases in the diameter of the hole.

It appears that the depth of the dent at the corners of the tube has the greatest effect on the peak load. The dent shape has a local effect on the buckling mode of the tube, but little effect on the buckling of subsequent lobes [37], and thus little effect on the mean buckling load.

3. EXPERIMENTATION

3.1 Introduction

The experimental program was initiated based on what was learnt from the literature, and intuitively where previous information was not available. As is typical for pioneering work, as the experimental program progressed, so the program was modified.

Prediction of some of the buckling characteristics of tubes, such as ultimate buckling load and mean buckling load, require the elastic properties of the tube material [2-7, 18-20, 27-28]. Tensile tests were thus performed.

It was shown in the literature[8-12,15,32,36-38] that different geometric imperfections introduced into tubes could change the buckling characteristics of the tube. Work on imperfections introduced by the use of explosives was not found, therefore preliminary experiments were required to determine the limitations that would be imposed on the type of imperfections available by the use of explosives.

Korneck[15] found that the formation of three lobes was sufficient for the calculation of the mean load. Abramawicz[26] developed an equation the predict the length of tube required for the formation of one lobe. The minimum tube length could therefore be predicted, although the geometric imperfections did change the size of the first lobe. The end effects were greater than expected and therefore in the case of the 100mm tubes, the length had to be extended.

Mild steel is a strain rate sensitive material[13], the literature[5,6,29] shows that increasing the velocity of crushing, increases the energy absorbed, and the mode of collapse was seen to be independent of loading rate[13]. Therefore quasi-static loading gives an accurate indication of collapse mode and a lower bound to the energy absorbed.

3.2 Test Specimens

All the specimens were cut from lengths of seam welded mild steel tubes. Tests were conducted on tubes of 50.8mm square section with a wall thickness of 1.2mm and tubes of 100mm square section with a wall thickness of 2mm.

Uniaxial tensile tests were carried out on the material as cut from the sides of the tubes, including a specimen along the weld seam of the tube. These were used to determine the static yield stress, ultimate tensile stress and percentage elongation of the material. The results of the tensile tests and the dimensions of the test specimens are detailed in appendix III.

3.3 Explosive Tests

Explosive tests were initially conducted to determine the limitations on the imperfections that could be created on square tubular specimens. In these tests a rectangular explosive configuration was used on the 50mm specimens.

Tests were performed to determine the effect that the mass of the explosive as well as the dimensions of the explosive had on the resulting deformations.

Tests were also performed using a flat circular explosive on the 100mm specimens to determine the effect of the mass and the diameter of the explosive on the deformations.

The notation used to describe the geometry of the different explosive configurations is shown in figure 3.1. The results are listed in Appendix IV.

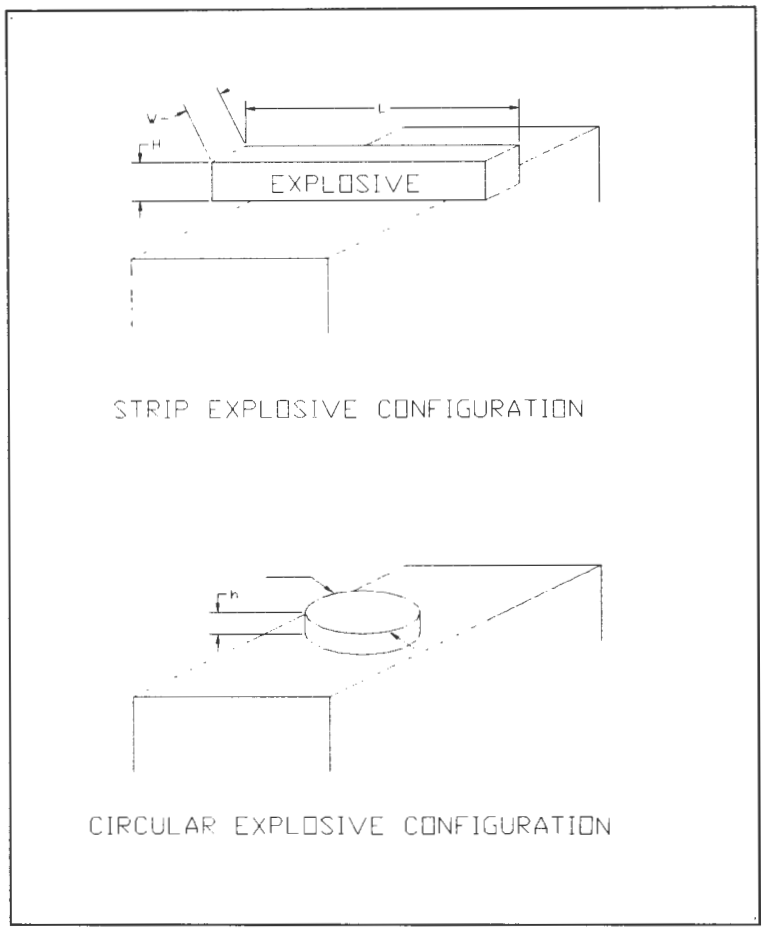

Fig 3.1 Geometry of explosive configuration

All the explosive tests were carried out on a ballistic pendulum in a reinforced blasting laboratory. The pendulum was a 100mm square tube suspended horizontally from the ceiling by 4 strands of steel wire. The pendulum was levelled with the aid of a spirit level, by means of the adjustable screws that connect the wires to the square tube. At one end of the square tube was a rig to clamp the test specimen. At the other end was a balancing mass positioned such that the centre of gravity of the pendulum is centralised and the four wire strands are each carrying the same load. A pen attached to the pendulum was used to record the motion of the pendulum. The motion of the pendulum can then be used to calculate the applied impulse.

The test specimens were clamped in a rig attached to the one end of the pendulum. The rig consisted of two U-pieces, 40 mm, long tightened on either side at the top of the specimen and two at the bottom of the specimen. The

amount of tightening was limited by the thin wall thickness of the specimens. Thus although the clamp did approximate a built in condition, under very large loading conditions a certain amount of global bending did occur particularly in the 50mm specimens (refer to figure 4.6). The distance between the clamps was 220mm. A diagram of the clamp, and a schematic of the clamped specimen are shown in figures 3.2 and 3.3 respectively.

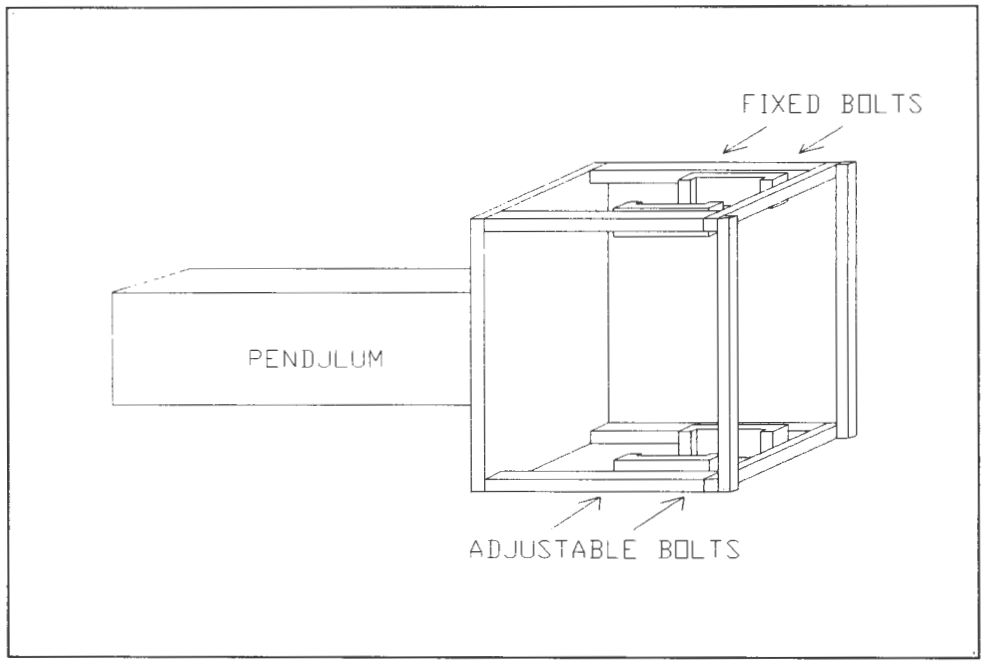

Fig. 3.2 Clamping rig for explosive tests

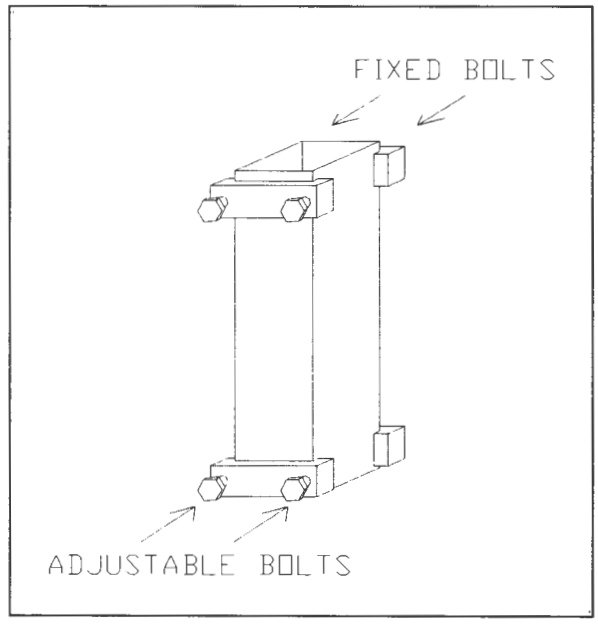

Fig. 3.3 Specimen clamped in the rig for explosive tests

The pendulum was used to record the impulse applied to the test specimen by the explosive load where required. The calculation of the impulse is shown in Appendix II.

The explosive used was PE4, a plastic explosive with a burn rate of between 6500 ms^{-1} and 7500 ms^{-1} and a density of approximately 1470 kgm^{-3}. The explosive was manipulated into specific shapes with the use of templates. The explosive was then placed on a piece of 12mm thick polystyrene which provided an air gap and prevented spallation. The polystyrene was stuck onto the test specimen with double sided tape.

The detonator was attached to the explosive in two different ways. For the strip configuration the detonator was positioned centrally on the strip and affixed with tape. For the circular explosive configuration 1g of explosive (the leader) was taped to the end of the detonator and this was pushed into the centre of the rest of the explosive. The leader was found to be required for complete detonation because the layer of explosive was thin.

3.4 Quasi - Static Loading of Mechanically Indented Tubes

The typical imperfections achieved by explosive loading were approximated with the use of mechanical indenters. The mechanically induced deformations were only tested on the 50mm tubes. All specimens were deformed symmetrically on two opposite sides (not on the welded seam) approximately at mid height of the tube. The tubes were then compressed quasi-statically using an Instron Tester. The critical loading characteristics are listed in Appendix V.

Tests were performed to compare the effects of:

- the depth of the dent at the corners of the tube
- the radius of the dent at the corners of the tube
- the diameter of centrally positioned holes

- combined holes and dents and the relations between the dimensions of the holes and dents,

The critical buckling characteristics that were compared were: the ultimate buckling load, the mean buckling load and the mode of collapse on the axial compression of the tubes.

All specimens were cut nominally 300mm long and the ends were faced off on a milling machine.

3.4.1 Indentation

The specimens were each clamped in a rig on the crosshead of the Instron Tester in order to prevent global bending of the specimen during denting. The indenter was attached to the load cell on the Instron Tester. The depth of indentation was measured by recording the displacement of the crosshead on a dial gauge. Once the dent had been formed, the specimen was turned over and reclamped in the rig. The process was repeated to create a dent of the same depth on the side opposite to the initial dent. In order to dent the specimens with holes, the spherical indenter was positioned symmetrically above the hole and then the specimen was clamped down.

The shapes of the indenters that were used are shown in figure 3.4

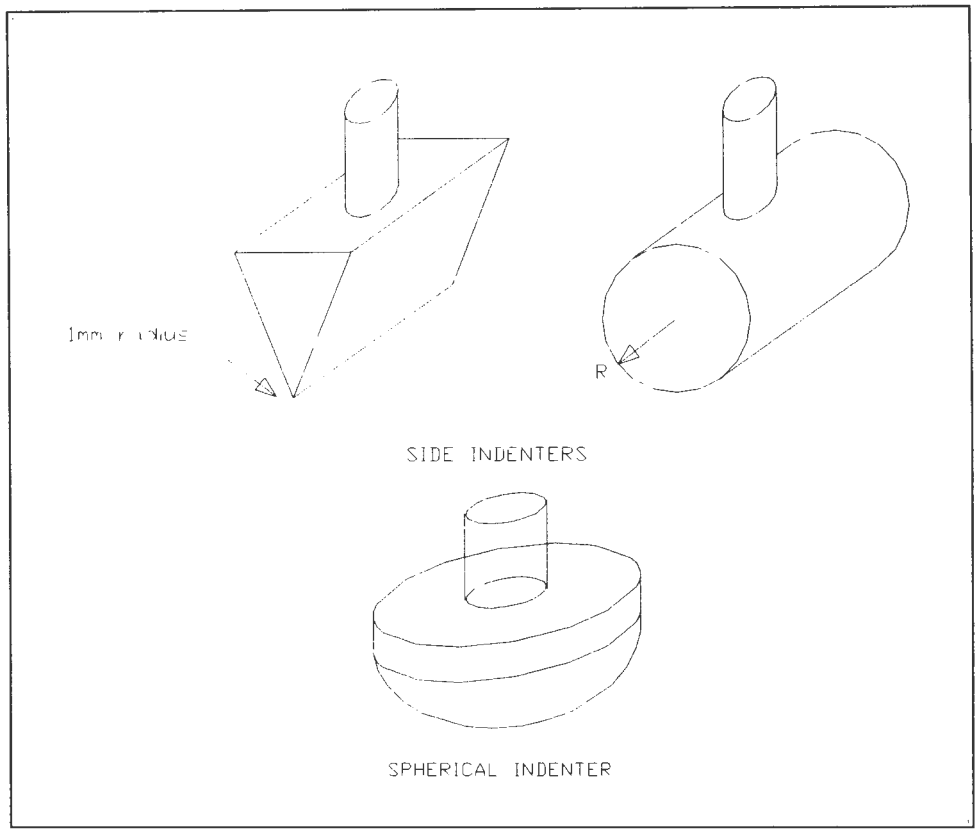

Fig 3.4 Mechanical Indenters

3.4.2 Quasi - Static Compression

The specimens were positioned between two parallel plates on the Instron Tester. The specimens were all loaded with a constant displacement of 0.2"/min (5.08mm/min). The resisting force of the tube was measured by the load cell. The results were plotted on a load-displacement curve on the Instron Tester. The maximum load rating on the load cell was 20 000 lbf (89kN)

3.5 Quasi - Static testing of Explosively Indented Specimens

In order to verify the results obtained from the quasi-static loading of mechanically indented specimens, the tubes were deformed explosively and then compressed. The specimens had to be deformed symmetrically on two sides of the tube. The two explosive charges positioned opposite one

another on the walls of the tube were detonated simultaneously by connecting the detonators in parallel with the power source.

Tests were conducted on the 100mm square tubing. Specimens of nominal lengths 300mm and 530mm were clamped into the rig on the ballistic pendulum. Explosive in the required circular configuration was attached to the specimen in a way similar to the first explosive tests. Two explosive charges were positioned on opposite sides of the specimen, perpendicular to the axis of motion of the pendulum. The pendulum was used merely to support the specimen during loading, and the impulse was not recorded.

The ends of the deformed specimens were then faced, and axially compressed quasi - statically on an Avery Compression Tester at the South African Bureau of Standards. A crosshead speed of 10 mm/min (0.39"/min) was used to compress the specimens. In a similar way to the Instron Tester, the results were recorded on a force - deflection curve.

A summary of the data obtained is listed in Appendix VI.

4. RESULTS

4.1 Tensile Test Results

The static yield stress and the static ultimate tensile stress were found from tensile tests performed on material taken from the square tubing. The results are tabulated in table 4.1

Table 4.1 Tensile Test Results

Tube	Static Yield Stress (σ_o) MPa	Ultimate Tensile Stress (UTS) MPa
AX	285	324
A	274	315
G	282	322
D	244	308
E	247	302

The letters in the first column correspond to the numbering system used to refer to the length of tubing from which the specimens were cut. The numbering was consistent throughout the testing. From the range of results obtained, it is clear that each length of tubing may be considerably different. An undeformed tube from each length was thus crushed quasi-statically to use as a standard comparison for the crushing results of deformed specimens.

4.2 Explosive Tests

An overview of the effect of the explosive configuration on the deformation shapes induced in thin walled square tubes was gained from the first series of explosive tests. The limitations imposed on the deformation shapes by the use of plastic explosive were determined. Figure 4.1a shows a photograph of tubes deformed by the explosion of a strip of plastic explosive. Figure 4.1b

shows diagramatically the critical measurements that were taken from the specimens.

The notation used for the geometry of the explosive mass was shown in figure 3.1 in the previous chapter.

Fig 4.1a Photograph of tubes deformed by a strip of explosive

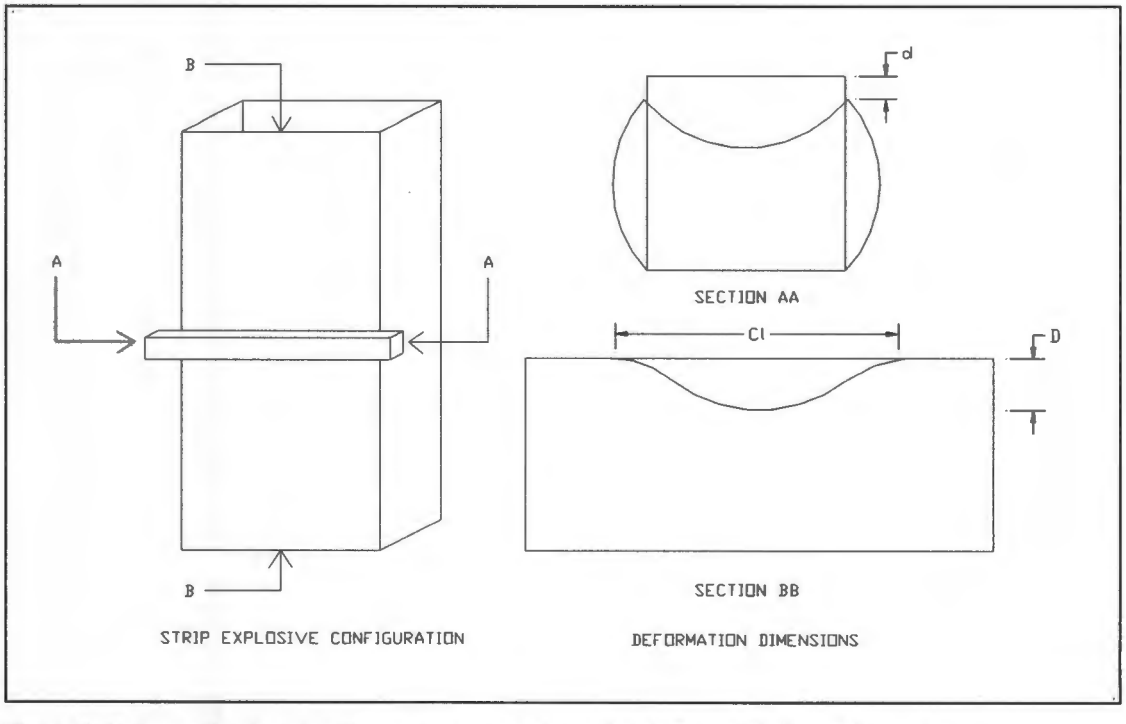

Fig 4.1b Schematic showing the measurements and notation of deformed specimens

4.2.1 The Effect of Explosive Configuration on the Applied Impulse

Although it is obvious that the mass of the explosive charge affects the impulse, it is interesting to note (as displayed in figure 4.2) that as the explosive strip becomes flatter and wider, the impulse for the same mass of explosive increased.

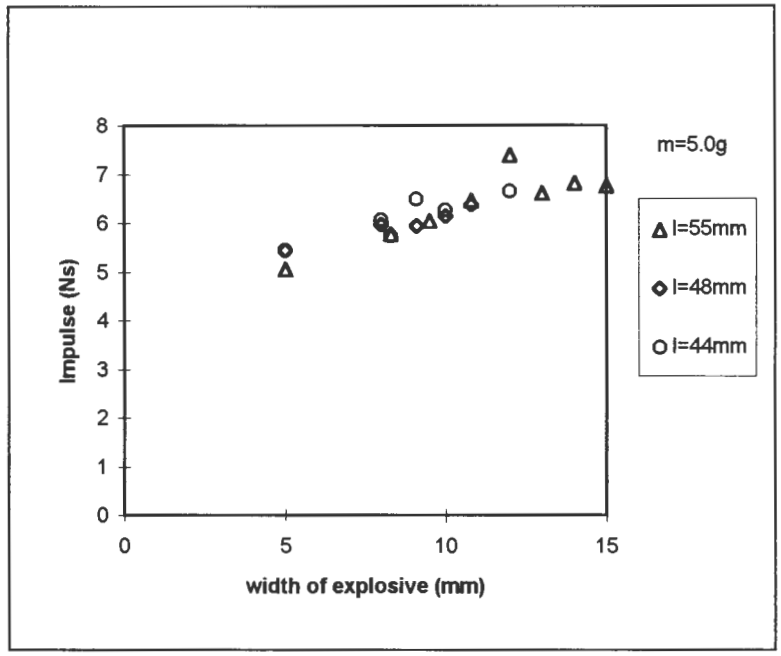

(a) Constant explosive mass of 5.0g

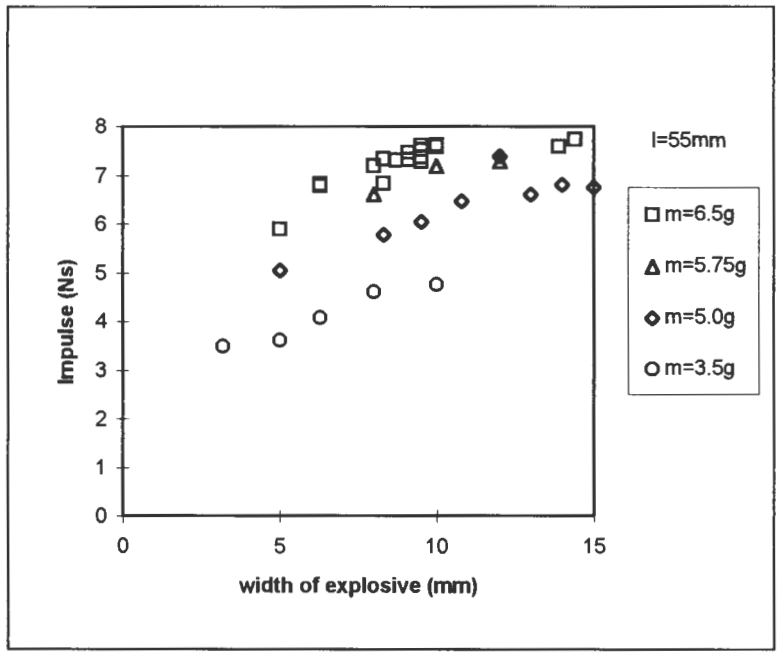

(b) Constant explosive length of 55mm

Fig 4.2 a-b The effect of explosive configuration on the impulse

4.2.2 The Effect of Strip Explosive Configuration on Deformation Characteristics

Figures 4.3 and 4.5 show the effect that the mass and configuration of the explosive have on the critical dimensions of the deformation of the tube. Note that the solid markers indicate specimens that tore, while the unfilled markers indicate specimens that displayed no evidence of tearing.

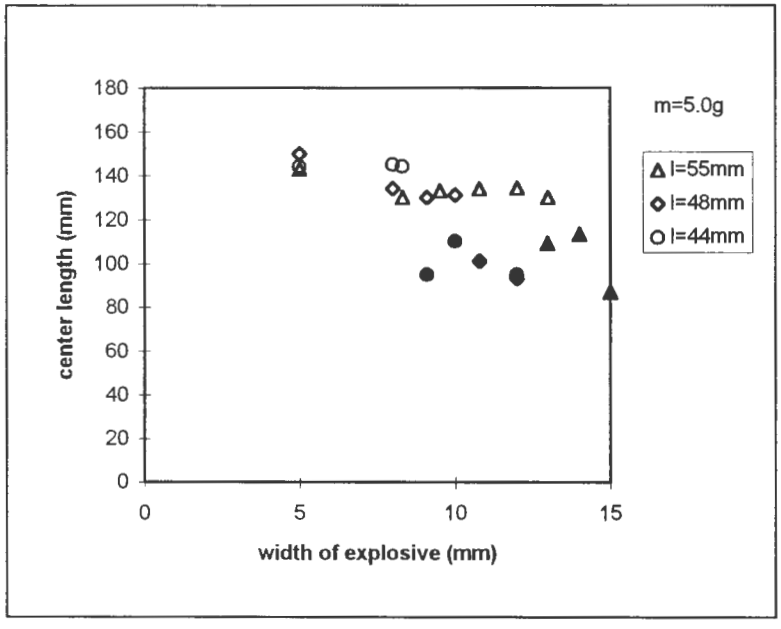

(a) Constant explosive mass of 5.0g

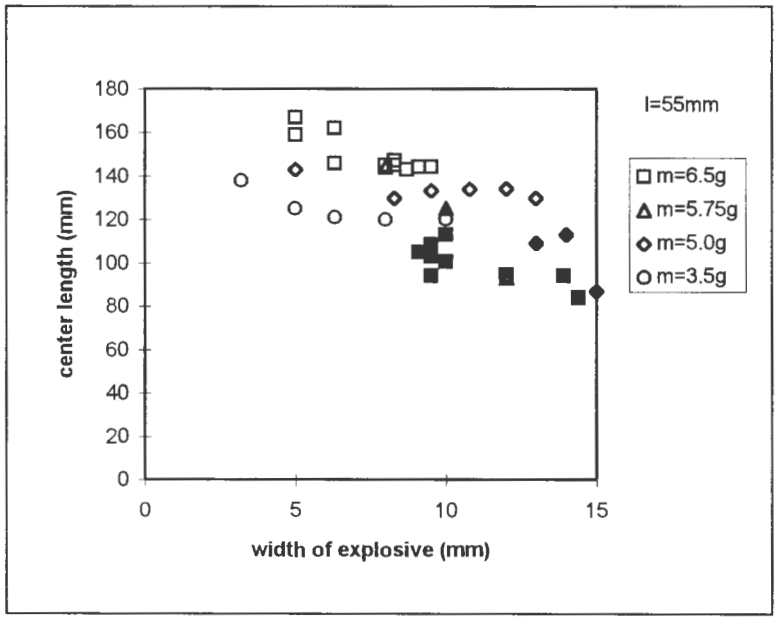

(b) Constant explosive length of 55mm

Fig 4.3a-b The effect of explosive configuration on the length of the deformation

Figures 4.3 (a) and (b) show that the geometric configuration had little effect on the centre length of the deformation in cases of specimens that did not tear. The length of the dent at the corners of the tube showed the same trends. The length of the explosive did however effect the occurrence of tearing. For shorter strips of explosive, the impulse was more concentrated and tearing occurred more readily. An increase in the explosive mass did effect the length of the deformation shape.

Untorn specimens showed an increased deformation length with an increased explosive mass. There was considerable scatter in the deformation lengths of torn specimens although it was clear that there was a considerable decrease in the deformed length in specimens that tore when compared to untorn specimens. This phenomenon is clearly illustrated in figure 4.4

Fig 4.4 Photograph showing the decrease in the length of the dent as the width of explosive is increased and the height decreased. The explosive mass (m) was 6.5g in all cases and the length of the explosive was 55mm.

Figures 4.5 (a) and (b) show the effect of explosive mass and configuration on the dent depth of deformed specimens. Note that the solid markers indicate specimens that tore, while the unfilled markers indicate specimens that displayed no evidence of tearing.

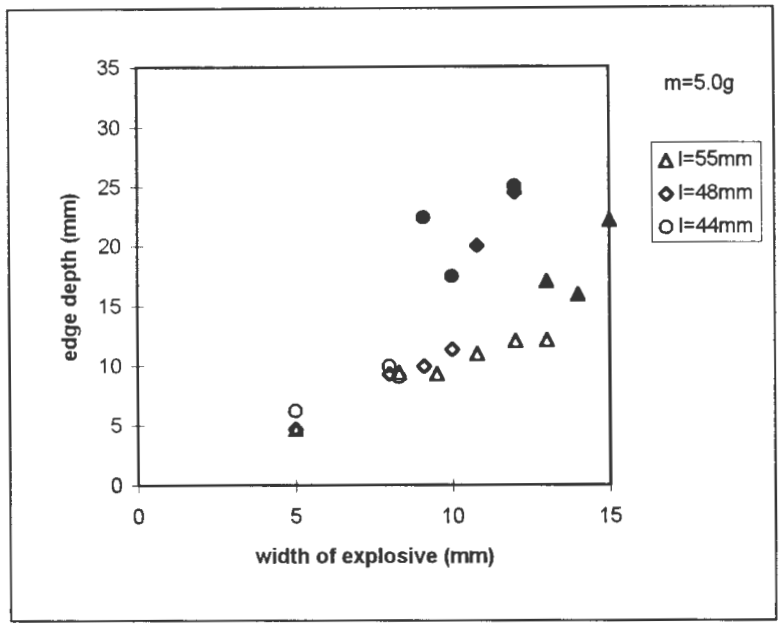

(a) Constant explosive mass of 5.0g

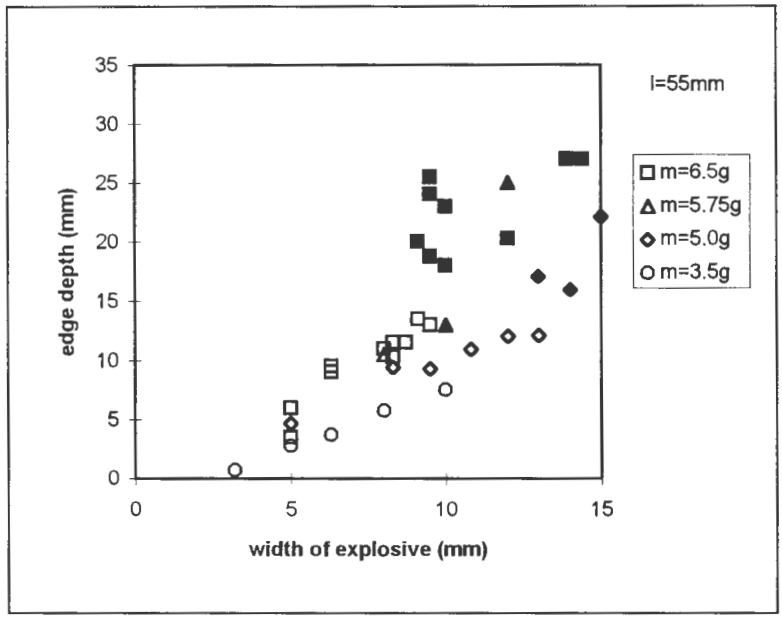

(b) Constant explosive length of 55mm

Fig 4.5 a-b The effect of explosive configuration on the dent depths

Figures 4.5 (a) and (b) show that the geometry of the explosive charge has a significant effect on the corner depth of the deformation. The centre depth of the dent showed a similar trend. The depth of the dents was increased as the width of the explosive strip increased (and hence the height of the explosive strip decreased). This is shown clearly in the photograph of the corner dent depth in the side view shown in figure 4.6.

The explosive length did not appear to have a considerable effect on the depth of the corner dent. Again the occurrence of tearing brought about a large scatter in the deformation dimensions as well as a sharp increase in the corner depth of the dents.

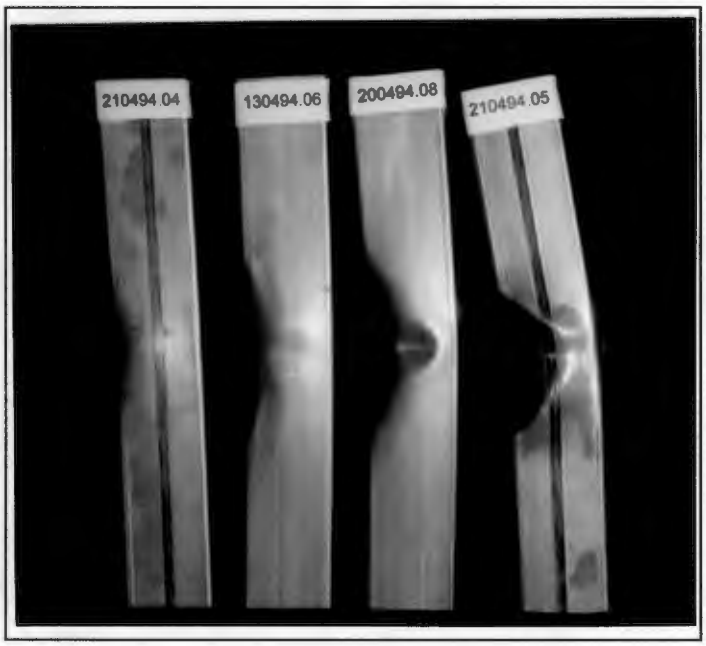

Fig 4.6 Photograph showing the increase in the dent depths for constant explosive mass but increasing width of explosive. The specimen on the far right tore.

4.2.3 The Effect of Circular Explosive Configuration on Deformation Shapes

Tests on circular plates loaded with a concentrated point charge were performed by Radford [40] An axisymmetric dished deformation shape with a central hole of diameter approximately equal to the diameter of the explosive

charge was formed. It was found that the circular hole could be formed with a smooth clean edge, although for large explosive masses 'petalling' of the edge did occur.

The use of flat circular explosive charges on 100mm square tubing was generally consistent with these observations. A central hole was formed at the location of the explosive. The holes were oval in shape, longer axially than laterally. The difference in the shape of the holes in plates and tubes can be attributed to a difference in the boundary conditions. The boundary conditions provided by the tubes are not symmetrical in both axes. The oval shaped holes can be seen in figure 4.7. The length of the hole was approximately the same size as the diameter of the explosive charge, except in cases where 'petalling' of the hole occurred. In most cases the width of the hole ranged from 30 - 40mm. Figure 4.8 shows the effect of the mass and the diameter of the explosive charge on the size of the hole.

The wall took on a dished shape, deepest in the centre and becoming less deep radiating outwards from the hole. The corners of the tube were also indented, but not as much as the rest of the tube wall because of their greater strength. The dent shape was thus not axisymmetric and the slope of the dent was much steeper in the lateral direction than in the axial direction.

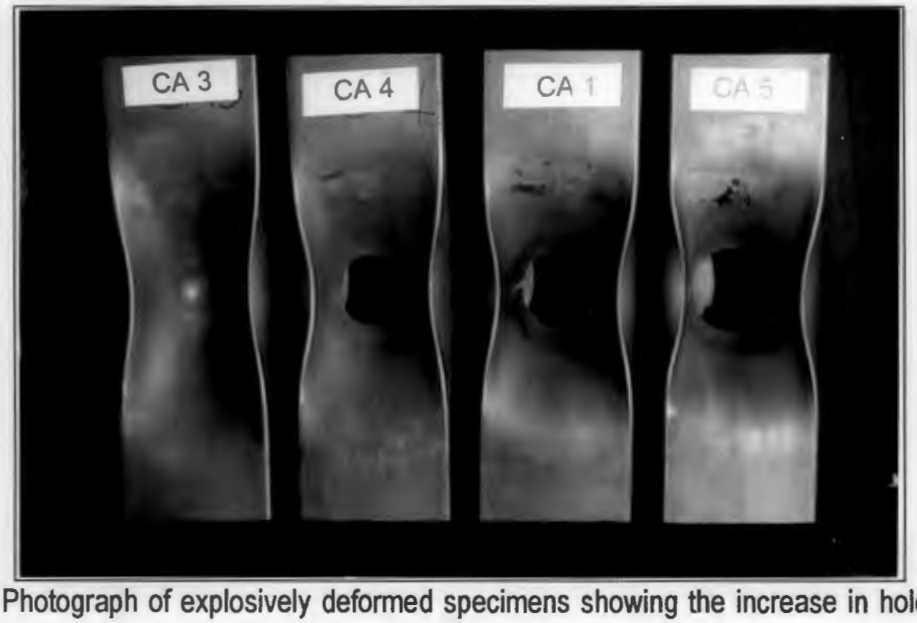

Fig 4.7 Photograph of explosively deformed specimens showing the increase in hole length. The diameter of the explosive charge was 48mm and the masses were: 9.0g; 9.5g; 12.0g; 14.0g from left to right

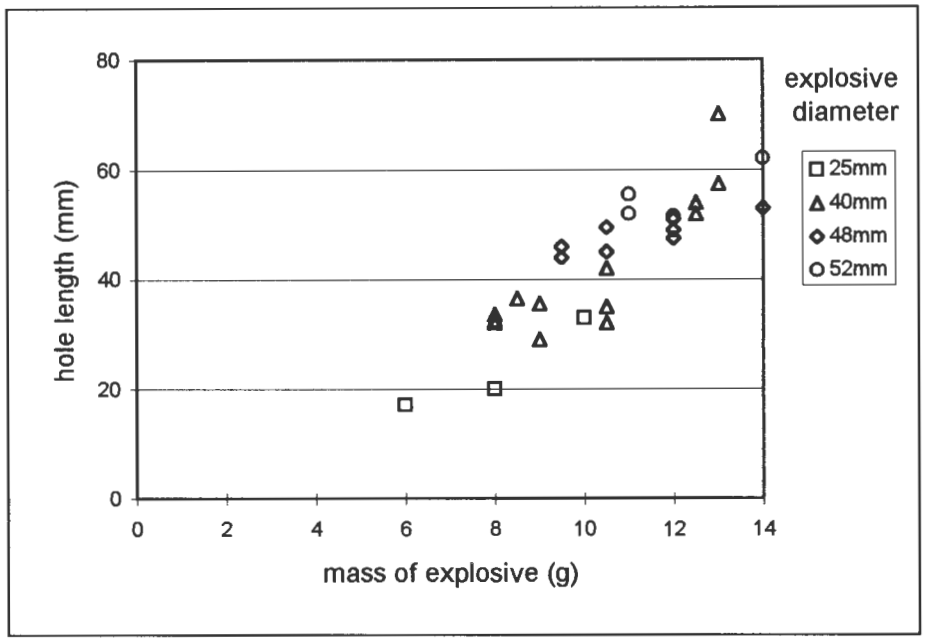

Fig. 4.8 The effect of the explosive mass and diameter on the size of the hole formed.

There was a large amount of scatter in the depth of the dents at the corners of the tubes. The general trend was an increase in depth with an increase in diameter of the charge for the same mass of explosive. Figure 4.9 clearly shows the large scatter of data.

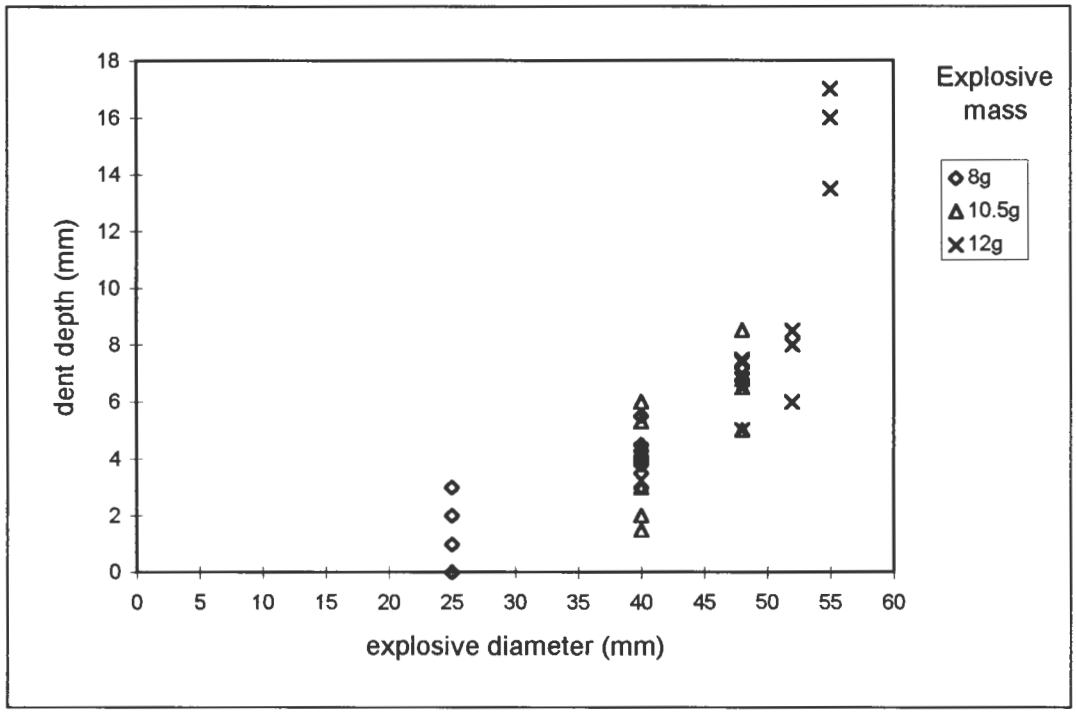

Fig 4.9 The effect of explosive mass and geometric configuration on the depth of the dents at the corners of the tubes.

In some instances, although the two charges were detonated simultaneously, it was assumed that one cap blew out momentarily before the other. From observations made after the experiment, it appeared that one cap hit the other cap before the second cap had blown out. The one cap was thus blocked it and preventing it from blowing out completely to form a hole. This did not appear to affect the collapse process of the tube.

4.3 Quasi - Static Loading of Mechanically Indented Specimens

4.3.1 Deformation Shapes

Side dents:

Different radii were imposed on the dents by using cylinders of different diameters. The parts of the walls not in contact with the denter folded gently inwards. The dent shape was not affected by the angle on the V-denter as the specimen was not in contact with the side walls of the indenter. The sides not directly indented bulged outwards. Tubes deformed with a 50mm diameter cylinder are shown in figure 4.10a

Spherical dents:

The deformations were of a concave shape, with centre deflections greater than the deflections at the specimen's corners. The deformation shape was more rounded in all respects and the transition between the parts of the walls in contact and out of contact with the denter were less defined than the cylindrically dented tubes. The deformation shapes gave a good resemblance to the explosively deformed tubes.

Holes:

The machining of holes in two opposite sides of the tube did not cause any measurable deflections in the walls of the tubes.

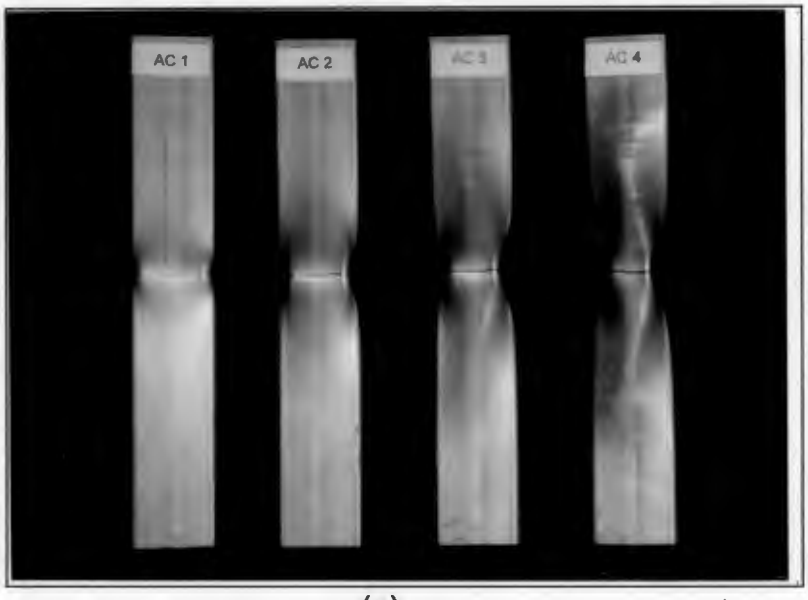

(a)

(b)

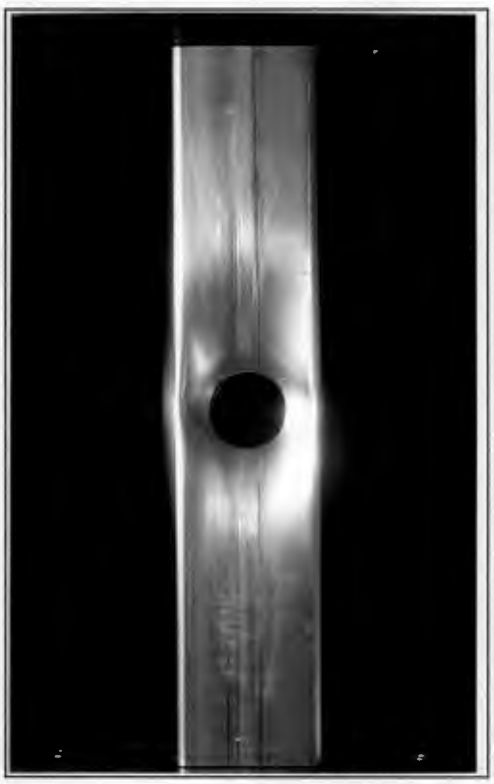

(c)

Fig 4.10 Photographs of specimens showing different deformations. (a) Cylindrical indentation (50mm diameter) to different depths, (b) Holed specimen, (c) Spherical indentation with a hole (the unholed deformations had the same dent shape).

Combined dents with holes:

A combination of spherical shaped dents with centrally positioned holes was produced. An example of the resultant deformation shape is shown in figure 4.10c.

4.3.2 Collapse Characteristics under Axial Loading

Load-deflection curves of the axially compressed specimens were generated on the Instron Tester. From each length of tube, one original undeformed tube was compressed to act as a standard for comparison. The other tubes were deformed locally by means of the mechanical indenters prior to compression.

The ultimate buckling load (P_{ult}) is the magnitude of the first peak load on the load deflection curve (refer to figure 2.2). This corresponds to the load at which plastic collapse begins.

The mean buckling load (P_{mean}) is calculated by the area under the load deflection curve (refer to figure 2.2).. For consistency between specimens the area of the curve was taken from the beginning of deformation of the tube to the last trough recorded on the load deflection curve. The corresponding amount of axial deformation was recorded, it included elastic deformation.

The geometry of the pre deformations affected the shape of the first lobe. If the shape was similar to the normal lobe shape (that which would form normally for an undeformed specimen) then there was no significant effect on the formation of subsequent lobes. However large changes in the shape of the first lobe tended to lead to instabilities that resulted in the unfavourable overall buckling of the tube. Overall buckling results in a lower absorption of energy.

The modes referred to in the tables are described as follows:

- **sp** :- Symmetric progressive buckling with no obvious tendency to bend over. Specimens G10 and G13 in figures 4.19 and 4.21 respectively show show the sp mode.

- **sspi** :- Skew symmetric progressive buckling caused by the formation of a small first lobe relative to the lobe size of an undeformed tube i.e. the distance between the plastic hinges decreased. The opposite lobes tended to fold one up and one down. This tended to force the tube skew, although not to the extent of overall bending, refer to specimen A2 in figure 4.17.

- **sspii** :- Skew symmetric progressive buckling caused by the formation of a large first lobe relative to the lobe size of an undeformed tube. The increased distance between plastic hinges required more folding space. In cases where there was insufficient folding space inside the tube, the two inward folding walls touched and reinforced one another. This prevented complete flattening of the lobe and instabilities occurred which caused skew buckling. Specimen G1 in figure 4.14 is an example of the sspii mode.

- **ebi** :- An extreme case of sspi. The tube went into overall buckling with a significant decrease in stroke.

- **ebii** :- An extreme case of sspii. The tube went into overall buckling with a significant decrease in stroke. Specimens G2 and G3 in figure 4.14 show the beginning of this buckling mode.

- **t** :- Tearing axially along the tube caused by the interlocking of cut edges tearing the sides apart. Refer to specimens A5 and A6 in figure 4.17.

4.3.3 The Effect of Side Dents

The results of the tests on the tubes that were mechanically deformed by indenting them with a cylindrical indenter before they were quasi - statically crushed are tabulated in tables 4.2 a-c.

Tables 4.2 a-c The effect of side dents

T 4.2 a Indenter radius: 1mm

Tube	Corner depth mm	Length mm	Pult kN	Phigh kN	Pmean kN	Mode
AA0	0	300	78	32	19	sp
AA1	5	300	34	34	20	sp
AA2	8.8	300	33			sspii
AA3	11.6	300	34			sspii

T 4.2 b Indenter radius: 15mm

Tube	Corner depth mm	Length mm	Pult kN	Phigh kN	Pmean kN	Mode
AA0	0	300	78	32	19	sp
AB1	2.8	300	40	34	22	sp
AB2	5.4	300	31	34	19	sp
AB3	7.6	300	31	28	19	sspii
AB4	8.7	300	33			sspii
AB5	11.3	300	34			sspii

T 4.2 c Indenter radius: 25mm

Tube	Corner depth mm	Length mm	Pult kN	Phigh kN	Pmean kN	Mode
AA0	0	300	78	32	19	sp
AC1	2.8	300	42	31	19	sp
AC2	6.1	300	32	31	20	sp
AC3	8.8	300	34	31	19	sspii
AC4	12	300	36			ebii

Figure 4.11 shows that the ultimate collapse load was decreased by introducing a dent into the specimen. As the depth of the dent was increased, the ultimate buckling load decreased. The ultimate buckling load decreased

asymptotically to a minimum at a dent depth of between 4.5mm and 6mm. This minimum ultimate buckling load coincided closely with the magnitude of the subsequent peak forces. The radius of the dent appeared to have no effect on the peak forces of the load deflection characteristics of the collapsing tube.

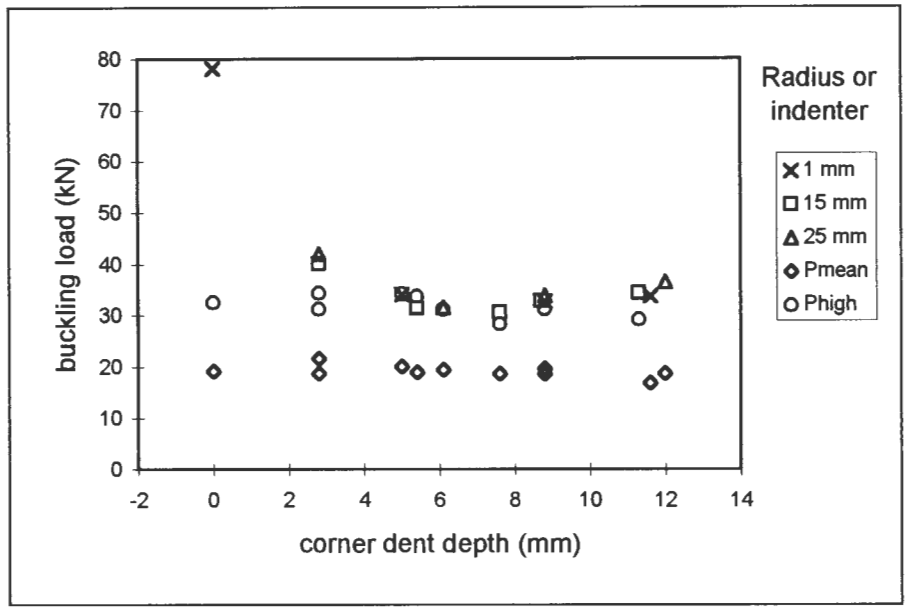

Fig. 4.11 The effect of the depth of the side dents on the critical buckling loads. The dent depths were measured at the corners of the 50mm square tubes with a 1.2mm wall thickness.

The mean crushing load is shown in figure 4.11 to be unaffected by either the depth or the radius of the dent.

Dents in the sides of the specimens affected the shape of the first lobe formed during the collapse process. If the dent depth was sufficiently large, then the walls on opposite sides of the tube touched and tended to reinforce one another. This resulted in a larger lobe with a greater distance between the plastic hinges than for undented specimens. Although the progressive buckling process did continue in most cases, for very large dent depths (greater than about 10mm) overall bending set in. Examples of specimens deformed to different dent depths of the same radius (25mm indenter radius)

are shown in figure 4.12. The radius of the dent had little effect on the mode of failure, although an increase in the dent depth increased instabilities in the buckling behaviour of the tube.

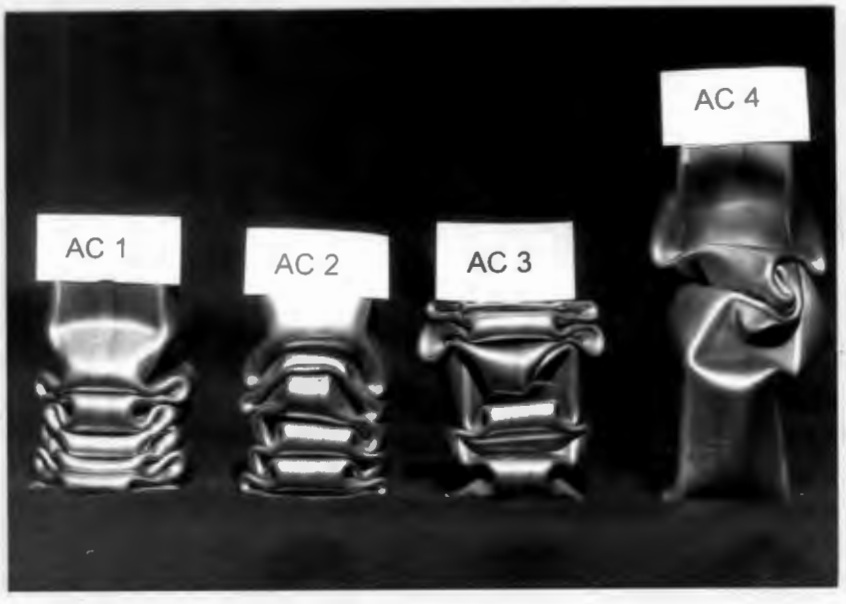

Fig 4.12 Photograph showing the effect of increasing the depth of the side dent. The dents were induced with a 25mm radius cylindrical indenter. The dent depth increases from left to right.

4.3.4 The Effect of Spherical Dents

The spherical indenter mechanically simulated the deformation shape of an explosively loaded square tube. The results of quasi-statically loading of the deformed tubes is tabulated in table 4.3

Table 4.3 The effect of spherical dents on the buckling characteristics of tubes

Tube	Corner depth mm	Length mm	Pult kN	Phigh kN	Pmean kN	Mode
G4	0	250	75	35	19	sp
G1	1.3	250	52	22	21	sspii
G7	1.5	250	53	30	16	sspii
G2	3.75	250	45	27	20	sspii - ebii
G6	4	250	45	26	21	sspii - ebii
G3	6	250	42	30	20	sspii - ebii
G5	6.5	250	41	30	20	sspii - ebii

Deformations induced in the shape of spherical dents caused a decrease in the ultimate collapse load of the tube. Neither the mean buckling load nor the magnitude of subsequent peaks changed appreciable. Figure 4.13 shows the above trends graphically.

The data shown in figures 4.11 and 4.13 is combined in figure 4.15 for the ultimate buckling load. It is clear that dents made by a spherical indenter do not decrease the ultimate load to the same extent as cylindrical indenters did. The results from Korneck [15] for sharp side indents are also included.

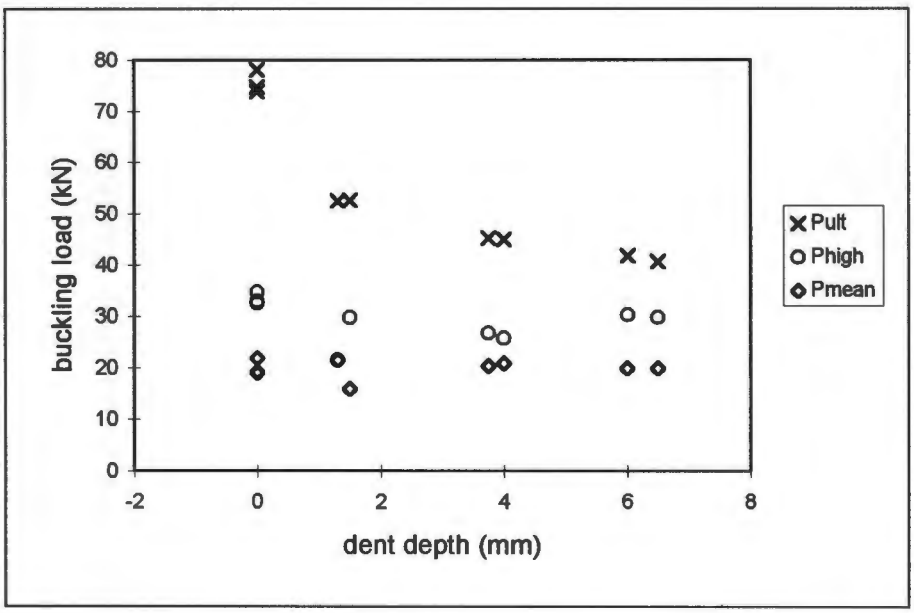

Fig. 4.13 The effect of the depth of the corner dent of spherically shaped dents on the critical buckling loads.

The opposite walls of the tube (those that were dented) made contact during the crumpling process. As the depth of the dent increased so the length of wall in contact increased. Again reinforcement occurred and progressive buckling of that section of the tube did not occur, although the rest of the tube did collapse before overall bending of the uncrushed section occurred. The increase in uncrushed lengths with increased dent depth is apparent in figure 4.14

Fig 4.14 Photograph showing the effect of increasing the depth of the spherical dent. The dent depth increases from left to right.

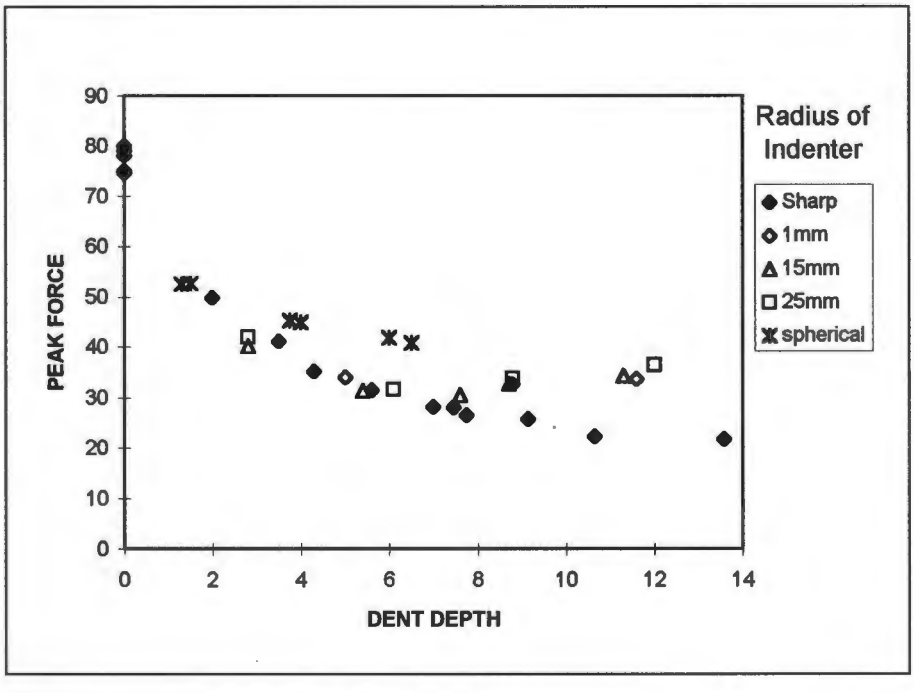

Fig 4.15 The effect of the depth of the corner dent on the ultimate buckling load.

4.3.5 The Effect of Holes

Two holes opposite one another were cut into the tube midway along the length. The tubes were then quasi - statically crushed. The results of the tests are tabulated below in table 4.4

Table 4.4 The effect of hole diameter on the buckling characteristics of square tubes

Tube	Hole diam mm	Length mm	Pult kN	Phigh kN	Pmean kN	Mode
A1	0	300	74	33	22	sp
G4	0	250	75	35	19	sp
G8	16	250	72		23	sspi
A2	16	300	69	30	23	sspi
A3	22	300	62	28	21	sspi
A4	25	300	51	31	21	sspi
G18	25	250	57	30	19	sspi
A5	32	300	52	25	22	t
A6	38	300	45	18	15	t

The introduction of round holes in the sides of a tube does decrease the ultimate buckling load of the specimen. The ultimate load decreased as the diameter of the hole increased as shown in figure 4.16. The mean and high peak loads appeared to be unaffected by holes smaller than 32mm. Holes with greater diameters resulted in tearing of the specimen rather than buckling and therefore the oscillating characteristic of the load displacement curve disappeared. Torn specimens (A5 and A6) are shown in figure 4.17.

The size of the first lobe formed during the collapse of the specimens was affected by the introduction of holes into the sides of the specimen. The distance between the plastic hinges of the lobe decreased. This tended to cause an instability in the folding mechanism and thus one lobe would fold upwards while the other folded downwards. This pushed the tube over and hence the skewness shown in the crushed specimens in figure 4.17

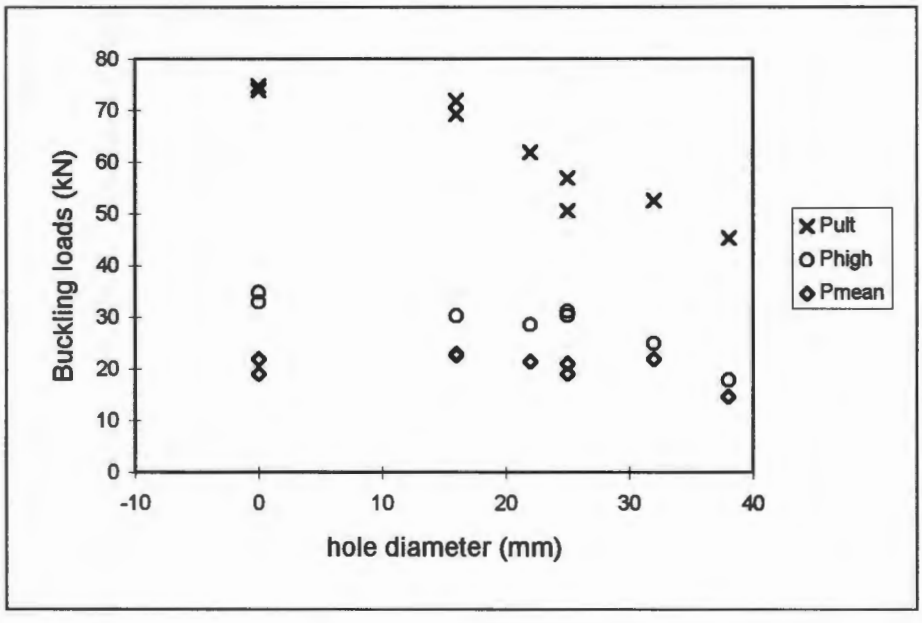

Fig 4.16 The effect of holes on the critical buckling loads.

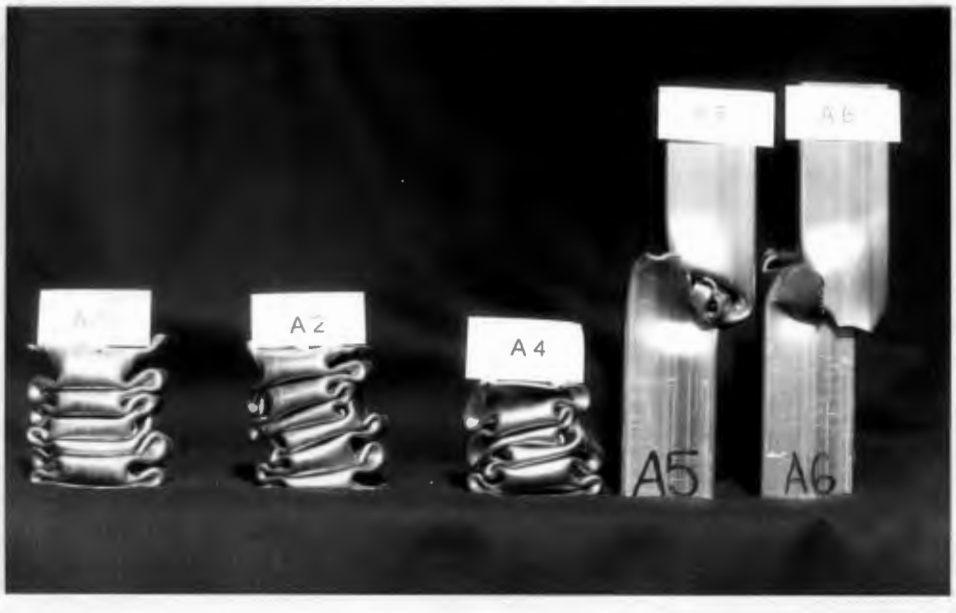

Fig 4.17 Photograph showing the effect of increasing the diameter of the hole. The hole diameter increases from left to right.

4.3.6 Effect of Combined Dents with Holes

The data tabulated below in tables 4.5 a - b shows the effect of different dent depths in combination with a hole of set diameter. The dent depth referred to is the depth of the corner dent.

Table 4.5 The effect of dent depth on the buckling characteristics of holed tubes.

T4.5a Hole Diameter: 25mm

Tube	Corner depth mm	Length mm	Pult kN	Phigh kN	Pmean kN	Mode
A4	0	300	51	31	21	sspi
G18	0	250	57	30	19	sspi
G9	6.3	250	36	26	20	sspii
G10	4	250	37	28	20	sp
G11	1.3	250	44	33	24	sspi

T4.5b Hole Diameter: 32mm

Tube	Corner depth mm	Length mm	Pult kN	Phigh kN	Pmean kN	Mode
A5	0 32	300	52	25	22	t
G12	5.9	250	33	34	17	sspii
G13	3	250	34	34	18	sp
G14	1.2	250	41	41		sspi

The addition of spherical dents to a specimen with holes decreased the ultimate collapse load further. Again it was clear that any change to the mean buckling load was negligible. A comparison of the ultimate buckling loads of dented and undented specimens with holes are shown in figure 4.18. The addition of dents decreased the ultimate buckling load to between 63% and 86% of the holed specimens without dents.

The addition of dents to holed specimens changed the way in which the first lobe formed considerably. It was noticed before in tests on specimens with holes that the hole decreased the distance between the plastic hinges in the

first lobe. It was found that for specimens with holes the addition of dents increased the size of the first lobe. For specimens with holes of the same diameter, increased dent depths increased the size of the first lobe. This trend is displayed in figure 4.19

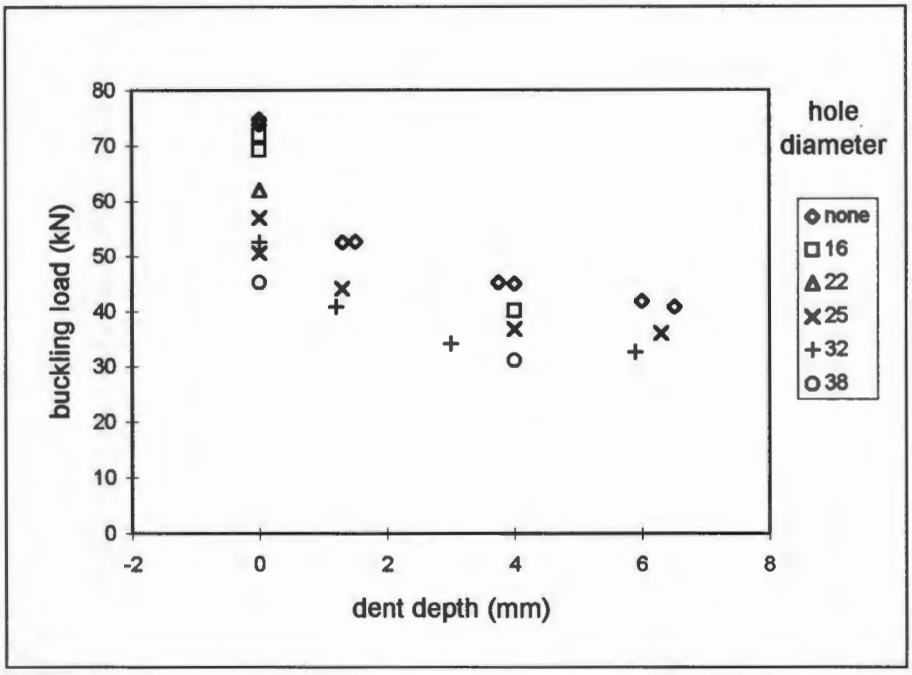

Fig. 4.18 The effect of dents on holed specimens.

Fig. 4.19 Photograph showing the effect of dents on the buckling mode of holed specimens. All specimens had holes of 25mm in diameter.

The data tabulated in tables 4.6 a - c show the effect of different hole diameters in combination with a set dent depth. The dent depth referred to is the depth of the corner dent.

Table 4.6 The effect of hole diameter on the buckling characteristics of spherically dented tubes.

T4.6a Corner Dent Depth: 1.5mm

Tube	Hole diam mm	Length mm	Pult kN	Phigh kN	Pmean kN	Mode
G1	0	250	52	22	21	sspii
G7	0	250	53	30	16	sspii
G11	25.7	250	44	33	24	sspi
G14	32	250	41	41		sspi

T4.6b Corner Dent Depth: 4mm

Tube	Hole diam mm	Length mm	Pult kN	Phigh kN	Pmean kN	Mode
G2	0	250	45	27	20	sspii-ebii
G6	0	250	45	26	21	sspii-ebii
G15	16.4	250	40	40		sspii
G10	25.7	250	37	28	20	sp
G13	32.5	250	34	34	18	sp
G16	38.4	250	31	31		sspi

T4.6c Corner Dent Depth: 6mm

Tube	Hole diam mm	Length mm	Pult kN	Phigh kN	Pmean kN	Mode
G3	0	250	42	30	20	sspii-ebii
G5	0	250	41	30	20	sspii-ebii
G9	25	250	36	26	20	sspii
G12	32	250	33	34	17	sspii

Considered from the aspect of adding holes to spherically dented specimens, figure 4.20 should be studied. The hole decreased the ultimate collapse load of spherically dented specimens to between 69% and 88% of the ultimate buckling load of the dented specimens without holes.

Although spherical dents increased the size of the first lobe, specimens dented to the same depth with holes of different diameters, showed that the hole decreased the distance between the plastic hinges i.e. the size of the first lobe decreased (see figure 4.21).

Specimens with moderate sized holes (25-32mm) and moderate dent depths (corner dent depths of about 4mm) crushed in a very favourable manner for energy absorption (G10 and G13 in figure 4.21 illustrate this). The large first lobe in specimens with large dents and small holes tended to destabilise the progressive buckling mode (G15). The unfavourable overall bending collapse in the tube was observed. An instability in specimens with large holes and small corner dent depths was also observed (G16). The effect of the hole dominated and these specimens tended to collapse in a mode similar to the holed but undented specimens (sspi).

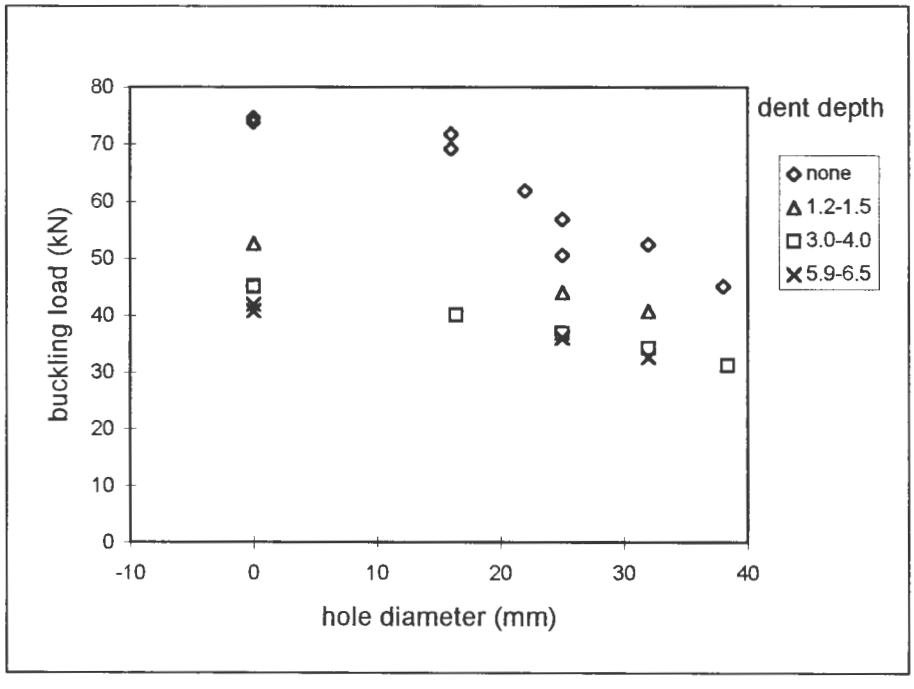

Fig. 4.20 The effect of holes on spherically dented specimens.

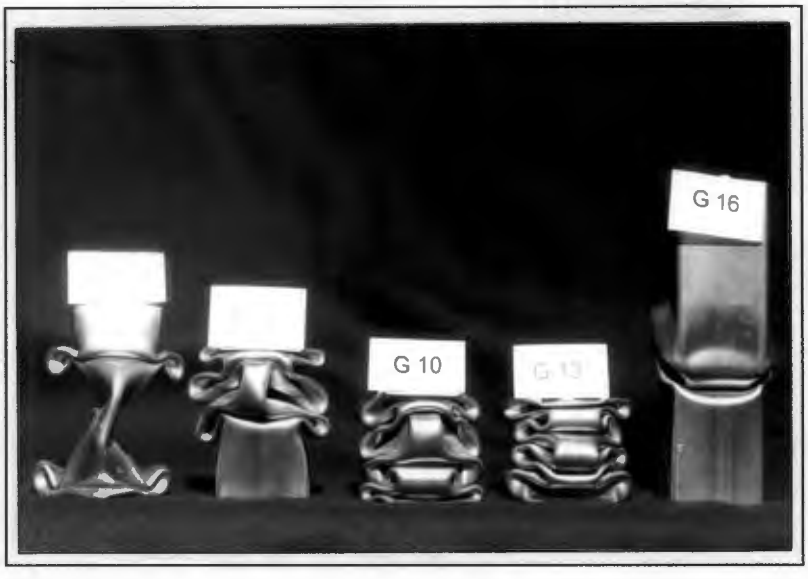

Fig. 4.21 Photograph showing the effect of holes on the buckling mode of spherically dented specimens. Sppecimen G2 did not have a hole. The diameter of the hole increases from left to right.

4.4 Quasi - Static Loading of Explosively Deformed Specimens

4.4.1 Collapse Characteristics under Axial Loading

The range of geometric imperfections introduced in the specimens tested decreased the ultimate buckling load to between 55% and 80% of the ultimate load of the originally undeformed tube. The imperfections did not appear to change the mean buckling load. The magnitude of the subsequent peak loads did appear to decrease in the more severely deformed specimens. The data is displayed in two different forms in figures 4.22 and 4.23.

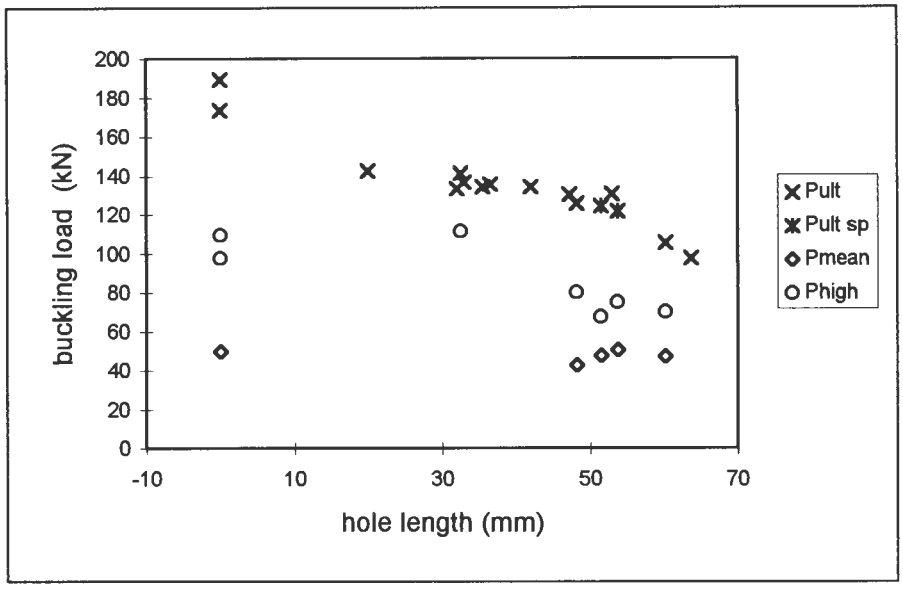

Fig 4.22 The effect of the length of the hole on the buckling characteristics of explosively deformed 100mm square tubes.

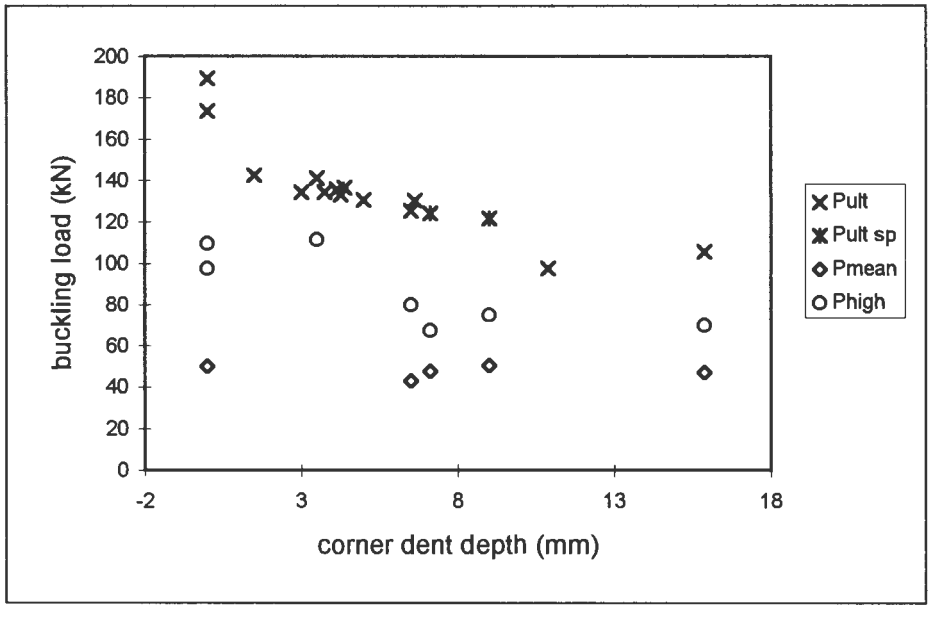

Fig 4.23 The effect of the depth of the corner dent on the buckling characteristics of explosively deformed 100mm square tubes. The tubes all had holes.

The mode of collapse was difficult to determine in the shorter specimens because of the influence of the boundary effects on the collapse of the tubes. It was decided that the only meaningful results that could be determined from these tests were the ultimate collapse loads. For the longer specimens it was found that symmetric progressive collapse, with no tendency for the tubes to skew to one side, did occur in two of the seven specimens. These two tubes are shown in figure 4.24.

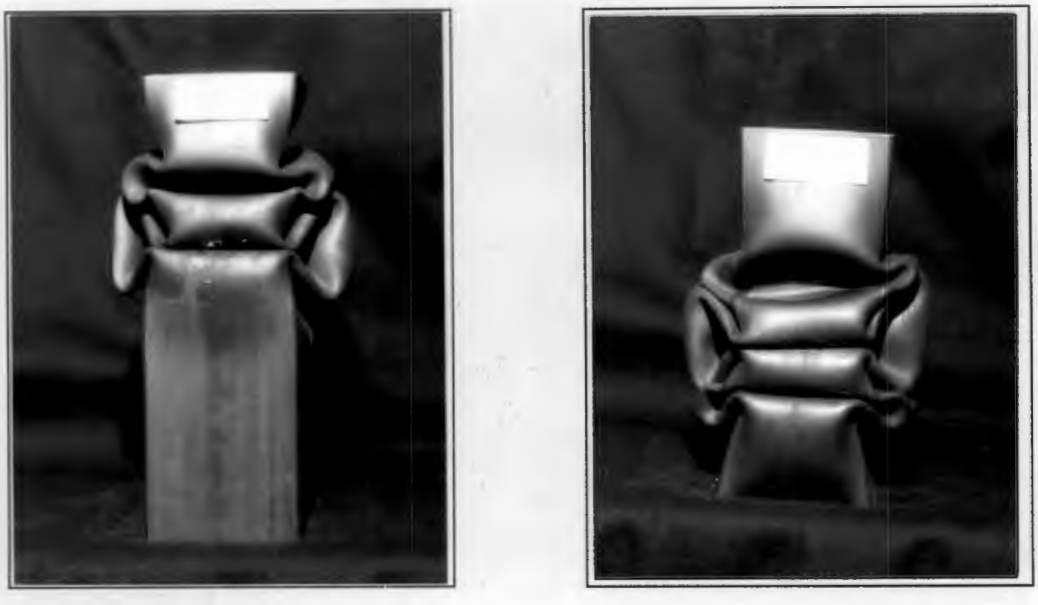

Fig 4.24 Photographs of the two specimens that buckled in the symmetric progressive mode (specimens EB5 and EB6).

Although most of the specimens did bend over and collapsed skew, it is interesting to notice that three lobes were formed during which the mean load was the same as the mean load of progressively buckled specimens, (see figure 4.25 for an example). These specimens would therefore have similar, favourable energy absorption characteristics to progressively buckled specimens for the length of stroke corresponding to the formation of three lobes.

Fig 4.25 Photograph of a specimen showing overall buckling. Notice the three fully formed lobes. (specimen EB4)

5. Discussion

5.1 Strip Explosive Configuration

It has been observed that the shape of the deformation imposed on the tube dictates the mode of collapse of the tube[8, 9]. This indicates that for stable symmetric progressive buckling to occur, the deformation shape should resemble the geometry of a lobe at the initiation of the lobe formation. The length of the deformation should therefore approximate the length of the natural wavelength of the tube. (The distance between three consecutive plastic hinges which make up one complete lobe is referred to as one natural wavelength ($2l$)). The half wavelength of the tube can be estimated by equation 4b for symmetric progressive buckling. This gives:

- $l \approx 27$mm for the 100mm tubes
- $l \approx 14.5$mm for the 50mm tubes

Half the length of the deformations induced in the 50 mm square tubes by strips of explosive, which would correspond to one half wavelength, was between 60 mm and 75 mm. The length of the deformations were far greater than the natural wavelength of the tubes.

The ultimate buckling load has been found to be affected by the amplitude of the deformation [8, 9, 15, 37]. Since most of the strength of the tube is derived from its corners it would appear that in terms of controlling the ultimate load, the depth of the dent at the corner would be most significant. The correlation between the effect of the corner dent depth and the uniform depth of the side dents on the ultimate buckling load (as evident in figure 4.15), appears to confirm this.

It therefore appears that the length of the deformation should be minimised while the depth of the dent at the corners of the tube can be used to control the magnitude of the ultimate buckling load.

5.1.1 Minimisation of deformation length

The geometric configuration of the explosive charge did not appear to affect the length of the deformation significantly, except in influencing the onset of tearing. It was found that shorter lengths of explosive strips caused tearing more readily than longer strips. The lengths of both the centre and corner dents were approximately constant for a constant mass with changes in explosive geometry for untorn specimens. Once tearing of the specimens ensued, there was a large amount of scatter in the length of the deformations, but the length was considerably shorter. This may indicate that tearing of the specimen could be advantageous.

The significant decrease in the deformation length with the onset of tearing would indicate the advantage of tearing a hole.

The corresponding increase in the deformation length with explosive mass would indicate that the smallest possible mass of explosive should be used.

5.1.2 Control of Corner Dent Depth

An increase in the mass of the explosive did result in a greater dent depth, however it is also clear that the same effect can be achieved by increasing the width and decreasing the height of the explosive configuration. A change in the length of the explosive charge did not have any great effect on the depth of the corner dent.

A low, wide explosive configuration increased the corner dent depth for a constant mass of explosive.

5.1.3 Optimum Explosive Mass and Geometric Configuration

The above discussion would seem to indicate that in order to impose a beneficial imperfection using an explosive charge to achieve the stable progressive buckling of a square tube a short flat explosive configuration should be used with the mass as small as possible while still achieving the required corner dent depth.

A flat circular shape for the explosive charge is consistent with the requirements of a short, wide configuration.

5.2 Circular Explosive Configuration

The shape of the deformation formed was not exactly the same as was found for circular plates loaded with a concentrated point charge[40]. The non axisymmetric boundary conditions of the square tubing, caused by the greater strength of the corners, resulted in an oval shape of the deformation.

There was a large scatter in the deformation dimensions. The large range of depths at the tube corners even in the same specimen, could have been due to either the position of the explosive charge or the detonator not being exactly centrally positioned, or the distribution of explosive in the charge not being completely even.

In the cases where one cap was prevented from blowing out completely by the other cap, the dished deformation shape of the tube wall did occur. The single hole in these specimens appeared not to affect the collapse mode of the tube adversely. In fact, one of the specimens that collapsed in the symmetric progressive mode (specimen EB6) had the one cap still attached

to the second unblown cap. Although this would reinforce the wall, the necking that had already taken place before the cap was blocked probably weakened the structure sufficiently to have the same effect as a hole would have done.

5.3 Energy Absorption Criteria

5.3.1 Ultimate Buckling Load

The ultimate buckling load is the maximum load that the column can support. If this load is exceeded the column will collapse. The load can be calculated from the classical formula:

$$P = \sigma_o A$$

where σ_o is the plastic flow stress

Abramowicz and Wierzbicki [28] defined the plastic flow stress as 92% of the ultimate tensile stress. Surko [9] used the von Karman postulate and defined the plastic flow stress as:

$$\sigma_o = \frac{2\alpha\sigma_y t}{C} \qquad \textit{...eqn 2.11a}$$

where α is a material constant defined by:

$$\alpha^2 = \frac{\pi^2 E}{12\left(1-\mu^2\right)\sigma_y} \qquad \textit{...eqn 2.11b}$$

and E is Young's Modulus taken to be 210 GPa for mild steel, μ is Poisson's Ratio taken to be 0.3 and σ_y is the tensile yield stress of the material.

The table 5.1 shows the predicted and measured ultimate loads for the different tubes tested.

Table 5.1 Comparison of predicted Ultimate Buckling Loads

TUBE	$\sigma_o=0.92\sigma_y$ [28] (kN)	von Karman (kN)	Experimental (kN)
A	68	81	74
G	69	82	75
D	222	213	174
E	217	214	190

The predicted values do give an idea of the magnitude of the ultimate buckling load. It is noted that the actual Young's Modulus of elasticity and Poisson's Ratio of the material, used in von Karman's theory were estimated as typical values for mild steel rather than being measured for each tube length.

When a thin walled square tube undergoes progressive buckling, the ultimate buckling load is considerably higher than the subsequent peak loads. In the applications considered for the energy absorbers being studied, ideal energy absorption would occur at a constant load. The oscillatory behaviour of the loads in a progressive buckling tube can be approximated by a constant mean load and is considered sufficiently constant to be used for energy absorption applications. The first peak force should however be reduced to approximately the magnitude of the subsequent peak forces.

It has been found previously that the introduction of a geometric imperfection causes the ultimate buckling load to decrease. The magnitude of the force can be controlled by the size and shape of the imperfection.

5.3.2 Mean Buckling Load

The total energy absorbed by the structure can be estimated by the product of the mean crushing load and the total distance crushed. It is therefore crucial that the mean crushing load is not significantly reduced by the

introduction of geometric imperfections. The mean static buckling load predicted for symmetric progressive buckling is given by equation 4a or 4c. The fully plastic moment was taken as $M_o = \frac{\sigma_o H^2}{4}$ and the plastic flow stress is $\sigma_o = 0.92\sigma_{UTS}$ [28]

Table 5.2 Mean Crushing Load (kN)

TUBE	Force predicted by eqn 4a	Force predicted by eqn 4c	Force measured for undeformed specimens
AX: σ_{UTS}=324MPa	19.4	20.7	19.4
A: σ_{UTS}=315MPa	18.9	20.1	21.2
G: σ_{UTS}=322MPa	19.3	20.6	22.2
D: σ_{UTS}=308MPa	54.4	58.6	-
E: σ_{UTS}=302MPa	53.3	57.4	50.0

It can be seen that either equation gives a good approximation of the mean crushing load. The specimens cut from length D were too short to give a meaningful indication of mean crushing load.

As was shown in the results, the mean crushing load did not change significantly between deformed and undeformed specimens. This is probably best explained by the reasoning that although the high peaks were lower, they were also wider and hence the area under the peaks was greater. This is illustrated in Appendix vii where three examples of the raw data have been reproduced. The shape of the first lobe was changed and this could result in an interference with the formation of the two lobes on either side of the first lobe.

Due to the fact that only the first lobe is significantly affected by the deformation [15, 37], the change in total energy absorbed due to a deformation is insignificant. Clearly the type of deformation is therefore not restricted by a loss in total energy absorption.

5.3.3 Total Energy Absorption

As discussed above, the total energy absorbed by the structure is dependent on its effective stroke. There are two criteria that affect the stroke:

- The amount that the lobes flatten, or the effective crushing distance. The more that the lobes flatten, the more the tube can compress, and hence the greater the amount of energy absorbed.

- The mode of collapse, or in the case of the progressively buckling of a tube, the stability of the collapse mode. Progressive buckling has been found to be an efficient energy absorbing collapse mode. Overall buckling results in far lower levels of energy absorption. In some of the tests conducted, although progressive buckling did start, the longitudinal axis shifted and overall bending of the tube occurred. In these cases the effective stroke was reduced to the distance over which progressive buckling occurred.

5.4 Quasi - Static Loading of Mechanically Deformed Specimens

5.4.1 Side Dents

Korneck[15] studied the effect of denting two opposite sides of a thin walled square tube on the ultimate collapse load of the tube. Standard 90° angle iron was used to form the dents. The collapse mode was found to stabilise into the symmetric progressive mode by the formation of the third peak force. The optimum ultimate collapse load was therefore determined to be the same load

as the third peak load, thus resulting in a constant amplitude of oscillation of the buckling load under progressive buckling collapse. Figure 2.10 shows that the optimum dent depth for mild steel square tubes with dimensions of 50x50x1.2mm is between 4mm and 5.5mm, or between 3.3 and 4.6 wall thickness'.

The optimum dent depth was extended to other tests and the dent depths used in the tests were in the optimum range and on either side of the range. Dents nominally 1.5mm, 4mm and 6mm were tested on the 50mm square tubes with wall thickness of 1.2mm.

The tests done by Korneck were extended in this project to include dents created with other indenters to introduce a range of dent radii. This was done because it is not possible to create a sharp dent using an explosive charge. The changes in dent radius were found to have an insignificant effect on the ultimate collapse load in the range studied. Some of the regularity of the folds was lost in the region of the deformation for deeper dents because of the change in the shape of the first lobe. Deeper dents forced the opposite walls closer together. The decrease in the width of the bulged sides resulted in a longer fold length. The first lobe did not always flatten as much as 'natural' lobes, and the stability of the collapse was compromised.

The tests were of limited value because the angles between the side walls retained their sharpness, while explosive charges caused a very rounded transition zone. The use of a spherical indenter was found to approximate the shape of an explosively induced dent far better.

5.4.2 Spherical Dents

The use of the spherical shaped indenter was to approximate the shapes of explosively formed dents. For purposes of comparison the dent shape was acceptable. The dent depth referred to is the depth of the dent at the corners.

The dents did significantly decrease the ultimate buckling load but not as much as dents of the same depth for the cylindrically indented specimens. This may have been because the rounded shape at the corners of the tube resisted the rotation of the hinge around the side of the tube.

The main problem with this type of dent was that the effective stroke of the tube was decreased by the order of one to two tube widths. The distance between the plastic hinges was increased to such an extent that the opposite walls of the first lobe touched. A large section of the tube was reinforced and thus did not fold flat. Progressive buckling did however continue on either side of the unbuckled portion of the tube before overall bending of the tube at the unbuckled section was induced.

Although the ultimate buckling load was decreased, the loss of effective stroke makes the introduction of spherical dents an unacceptable solution

5.4.3 Holes

The introduction of holes is another documented way to reduce the ultimate buckling load of the tube [9 - 12]. The use of von Karman's postulate predicted that holes in the side walls of the tubes had to be of diameters greater than 31mm for the 50mm square tubes and 66mm for the 100mm tubes in order to decrease the ultimate collapse load. Two holes, one in each wall opposite one another, of diameters of 16mm did not have an effect on the ultimate buckling load of the 50mm square tubes, but diameters of holes as small as 22mm holes did decrease the ultimate load.

The holes had a lesser effect on the ultimate buckling load of the tubes than the dents that affected the corners of the tube. This was to be expected because of the greater load carrying capacity of the corners. Specimens with holes of which the diameters were large enough to effect the ultimate load sufficiently, failed by tearing. The edges of the holes interlinked and tore

each other. The occurrence of tearing instead of buckling is the reason for the slight decrease in the mean load and the absence of subsequent peaks.

The most significant change induced by the introduction of holes into the tube walls was in the shape of the first lobe. The distance between the plastic hinges decreased and a smaller lobe formed. It appeared as though the effective tube width was decreased and hence the distance between the plastic hinges decreased.

The small decrease in the ultimate buckling load is considered to be insufficient. There is a high probability of skew collapse of the tube as the size of the hole is increased.

5.4.4 Combined Dents with Holes

The combination of holes and dents decreased the ultimate buckling load more than either of the imperfections individually.

The changes in the distance between the plastic hinges for specimens with either holes or dents was also consistent with the changes in combination, and the effects were additive. Increasing dent depths increased the distance between the plastic hinges. Increasing hole diameters decreased the distance between the plastic hinges.

Specimens with large holes and small dents deformed in a similar way to holed specimens. The small lobes led to the tube buckling skew which is useless for efficient energy absorption. In specimens with small holes and large dents, the dent dominated the shape of the first lobe. In the same way as for spherically dented specimens there was a reduction in the possible length of the stroke. The uncrushed length was however significantly shorter than the uncrushed length of the specimens without holes. This means that

although not ideal, tubes with large dents and small holes could be considered for energy absorbers.

The above discussion indicates that there is an optimum combination of dent depths and hole diameters that would result in the formation of the first lobe equal in length to the natural wavelength of the tube, while still having sufficient effect in decreasing the ultimate load. This optimum was observed to occur at a hole diameter of between 25mm and 32 mm (50% -64% of the width of the tube) and a dent depth of 4mm (about $3^1/_3$ wall thickness'). These dimensions were found for 50mm square mild steel tubes with a wall thickness of 1.2mm. The effect of different tube dimension was not adequately studied.

The magnitude of the ultimate buckling load decreased as the dimensions of the deformation increased.

An increase in the diameter of the hole decreased the distance between the plastic hinges of the first lobe. An increase in the depth of the dent increased the distance between the plastic hinges of the first lobe. This phenomenon as used to control the size of the first lobe and consequently the stability of the symmetric progressive buckling mode.

5.5 Quasi-Static Axial Loading of Explosively Deformed Tubes.

Two series of tests were done on 100mm square mild steel tubing with a wall thickness of 2mm. Lengths of tubing of 300mm were used in the first tests. These tubes proved to be too short. Although the ultimate buckling loads were found, the edge effects interfered with the formation of the subsequent lobes. The deformation mode and mean collapse load could therefore not be determined. Lengths of tubing of 530mm were then tested and the failure mode was considered.

The introduction of the deformations decreased the ultimate peak force. Most of the specimens had a peak force which lay in a band of between 65% and 80% of the peak load of the original, undeformed specimens. Figures 4.22 and 4.23 show that for the range of deformations tested, the ultimate buckling load was decreased compared to the undeformed specimens, but was not significantly different for the different deformation dimensions tested. The two exceptions observed were both very largely deformed and the holes formed were not regular oval shaped. The edges of the holes tore radially, forming what resembled large petals. These two specimens did not fail in the desired mode. *The reduction in the ultimate buckling load is therefore restricted by the requirement of symmetric progressive buckling.*

The mean crushing load was found to remain fairly constant as was expected from all previous tests. The magnitude of the peak loads (P_{high}) was seen to decrease for cases where the deformation dimensions were very large. This may be a misleading result as the crushing distance corresponded to the formation of only three lobes, although Korneck[15] did observe that the peaks stabilised after the formation of three lobes. However, if the amplitude of the oscillations decreased for the same mean crushing force then the load oscillations would be reduced and the overall force more constant.

In the second series of tests, of the seven deformed specimens, two deformed by perfect progressive buckling. The two specimens that crushed favourable showed that a diameter of about 53mm ($^{D}/_{C} = 0.53$) and a corner dent depth of between 7mm and 9mm ($3.5 < d/t < 4.5$) was optimum for the tubes tested. Further tests would be required to determine interpolation for other materials and tube dimensions.

The specimens that did not undergo pure symmetric progressive buckling tended to skew after the formation of three lobes. The significance of the formation of the three efficient energy absorbing lobes is that if the use of numerous pairs of explosive charges is considered, this gives an indication of

the optimum distance between charges. i.e. The charge pairs should be placed three natural wavelengths apart.

It was confirmed that the introduction of spherical dents with centrally positioned holes induced explosively provided an adequate solution. Further investigation is required in order to optimise the deformation dimensions for specific tube dimensions. It is recommended that a hole approximately half the width of the tube be used, and that the dent at the corners of the tube be about 3 - 4 times the wall thickness of the tube.

6. CONCLUSIONS

6.1 Strip Explosive Configuration

The following conclusions are concerning the limitations imposed on deformation shapes induced by explosive charges:

- The dent shapes were rounded, and the sharp edges that could be induced mechanically, could not be reproduced explosively.

- The length of the dent was much larger than the natural wavelength of the tubes (of the order of five times larger). The deformation length should thus be minimised.

- The depth of the corner dent, which is believed to control the magnitude of the ultimate buckling load, could be controlled by the mass and geometric configuration of the explosive.

6.1.1 Minimisation of the Dent Length

6.1.1.1 The length of the dent was significantly less in all the specimens that tore. For the same mass of explosive, tearing was induced more easily for shorter lengths of explosive charge.

6.1.1.2 The length of the dent was decreased as the mass of explosive was decreased.

6.1.1.3 The length of the dent was minimised as the height of the explosive charge was minimised (with a corresponding increase on the width of the explosive). The minimum height of explosive required for complete detonation was about 2.5mm.

6.1.2 Control of the Corner Dent Depth

6.1.2.1 The depth of the corner dent was increased with an increase in the mass of explosive used.

6.1.2.2 The depth of the corner dent was increased with a decrease in the height of the explosive charge for a constant mass of explosive.

6.1.3 Optimisation of the Explosive Mass and Geometric Configuration

The conclusions drawn in sections 6.1.1 and 6.1.2 indicate the following:

6.1.3.1 The minimum possible mass of explosive should be used.

6.1.3.2 The height and length of the explosive should be minimised with a corresponding increase in the width of the explosive.

6.2 Circular Explosive Configuration

The above conclusions would suggest that a flat round shaped explosive configuration is optimal.

6.3 Energy Absorption Criteria

6.3.1 The ultimate buckling load was found to be decreased by the introduction of a deformation. It was confirmed that the magnitude of the ultimate buckling load could be controlled by the size of the deformation induced.

6.3.2 It was found that the mean buckling load was not significantly affected by the introduction of deformations if the deformations did not change the mode of buckling, i.e. if symmetric progressive buckling did occur.

6.3.3 The total energy absorbed by the specimen was significantly decreased by the onset of Euler buckling. Deformation shapes or dimensions that induce Euler buckling should thus be avoided.

6.4 Quasi-Static Loading of Mechanically Deformed Tubes

Tubes in which deformations were mechanically induced were quasi-statically crushed. The following conclusions were drawn:

6.4.1 Side Dents

Although the sharp edges of the side dents mechanically induced could not be reproduced explosively, the tests did give an indication of the corner dent depth required for control of the ultimate buckling load. For the 50mm square mild steel tubes with a wall thickness of 1.2mm that were tested, the optimum dent depth appeared to be between 4 and 5.5mm.

6.4.2 Spherical Dents

6.4.2.1 The ultimate buckling load was decreased by the introduction of a spherical dent. The decrease in the ultimate buckling load was not as great as for the side dents.

6.4.2.2 The distance between the plastic hinges of the first lobe appeared to be greatly increased. The length of the stroke was thus significantly shortened by the incomplete formation of the first lobe and the consequently uncrushed length of tube. The uncrushed length of tube increased with an increase in the depth of the dent.

Spherical dents were thus found to be an unsatisfactory solution due to the decrease in the effective stroke.

6.4.3 Holes

6.4.3.1 The presence of holes in the walls of the tubes decreased the ultimate buckling load to some extent. The magnitude of the ultimate buckling load did decrease with increasing hole diameter.

6.4.3.2 The diameter of the hole was limited by the onset of tearing of the side walls during crushing. The tearing was induced by the interlocking of the cut edges.

6.4.3.3 The presence of holes appeared to decrease the distance between the plastic hinges of the first lobe. This led to skewing of the tube, and in extreme cases, to Euler buckling.

Holes were found to offer insufficient decrease in the ultimate buckling load and were thus discarded as a potential solution.

6.4.4 Holes and Spherical Dents

6.4.4.1 The combination of spherical dents with centrally positioned holes decreased the ultimate buckling load. This decrease in the ultimate buckling load was found to be greater for the combination of hole and spherical dents than for either deformation individually.

6.4.4.2 The apparent increase in the distance between the plastic hinges of the first lobe induced by the presence of spherical dents, and the decrease caused by the holes, appeared to be compensatory. An optimum should thus exist for which the two negative effects eliminate one another. This would result in a first lobe of length equal to the natural wavelength of the tube. The instabilities that resulted from a change in lobe size would be eliminated and "perfect" symmetric progressive buckling would occur. For the 50mm square mild steel tubes with a wall thickness of 1.2mm that were tested, the

optimum appeared to occur for a hole diameter of 25mm and a dent of depth at the corners of 4mm.

The combination of spherical dents with centrally positioned holes may offer an extremely satisfactory solution.

6.5 Explosively Induced Dents with Centrally Positioned Holes

6.5.1 It was found that circular holes could be induced in the centre of spherical shaped dents by using a flat, round explosive configuration. The diameter of the hole was found to be approximately the same diameter as the diameter of the explosive charge. The depth of the dent could be controlled by the mass of the explosive.

6.5.2 The ultimate buckling load of the tube was significantly reduced.

6.5.3 Typical symmetric progressive buckling was found to occur for a deformation with a hole of diameter of approximately 53mm (Half the width of the tube), and a corner dent depth of between seven and nine mm for the 100mm square mild steel tubes with a wall thickness of 2mm.

6.5.4 The formation of the three efficient energy absorption lobes that occurred in specimens that failed by Euler Buckling, indicates that pairs of charges positioned in series, and spaced at a distance equivalent to three natural wavelengths apart, should be investigated further.

7 CONCLUDING REMARKS

The effect of a number of deformation shapes explosively induced in thin walled square tubes was studied in the context of energy absorption. Of all the deformation types presented in the study, spherical shaped dents with a centrally positioned hole offer the best energy absorption characteristics: the ultimate buckling load can be significantly decreased; the mean buckling load remains unchanged; and the symmetric progressive buckling mode can be induced.

Spherical shaped dents with centrally positioned holes can be induced explosively by flat, circular explosive charges. The diameter of the hole formed was approximately equal to the diameter of the explosive charge used. The optimum diameter for symmetric progressive buckling appears to be about half the width of the tube. (The tubes tested showed that a 25mm hole diameter was optimum for the 50mm tubes, and a 53mm diameter was optimum for 100mm tubes.) The mass of the charge was used to control the depth of the dent. A dent depth of between 3.5 and 4.5 wall thickness' was shown to be optimum for the tube dimensions tested.

Optimisation of the exact deformation dimensions required for specific energy absorption members is required. The mass of explosive required to produce the necessary deformation dimensions is dependent on the type of explosive used.

The use of pairs of explosive charges in series positioned three natural wavelengths of the tube apart is proposed. The proposition has not yet been investigated.

The study was limited to quasi-static crushing of tubes. Although evidence indicates that dynamic effects are similar to static effects, it is strongly recommended that dynamic tests be conducted.

REFERENCES

1. W. Johnson and A.G. Mamalis,'Crashworthiness of Vehicles. An introduction to aspects of collisions of motorcars, ships, aircraft, and railway coaches.' Mechanical Engineering Publishers Ltd. London (1978)

2. A.G. Pugsley and M. Macaulay,' The large scale crumpling of thin cylindrical columns.' *Q. J. Mechanics Appl. Math.*,**13**, pp. 1-9 (1960)

3. J.M. Alexander, 'An approximate analysis of the collapse of thin cylindrical shells under axial loading', *Q. J. Mech. Appl. Math.*, **13**, pp. 1-9 (1960)

4. W.Abramowicz and N. Jones, 'Dynamic axial crushing of square tubes,' *Int. J. Impact Engng*, Vol **2,** No **2,** pp. 179-208, (1984)

5. W. Abramowicz and N. Jones, 'Dynamic axial crushing of circular tubes,' *Int. J. Impact Engng*, Vol **2,** No **3,** pp. 263-281, (1984)

6. W. Abramowicz and N. Jones,'Static and dynamic axial crushing of circular and square tubes.' Metal forming and Impact Mechanics, (Edited by S.R. Reid) pp 225-247. Pergamon Press Oxford. (1985)

7. T. Wierzbicki, S.U. Bhat, W. Abramowicz, and D. Brodkin, ' Alexander Revisited - A Two Folding Elements Model of Progressive Crushing of Tubes.' *Int. J. Solids Structures* Vol **29** No. **24** pp.3269 - 3288, (1992).

8. T. Schriever and J. Helling, 'Zum Einfluβ gezielt eingebrachter geomertischer Imperfektionen auf das Verformungsverhalten von Langstragerstrukturen.'

9. W. Surko, 'Crushing Strength of Box Columns with Partially-Damaged Plating.' *Int. J. Mech. Sci.* Vol **33**, No. **12**, pp 1017 - 1028, (1991)

10. S. Toda, 'Buckling of Cylinders with Cutouts under Axial Compression.' *Exp. Mech.* pp 414 - 417 (1983)

11. K. Kormi, D.C. Webb, and P. Montague, 'Crash Behavior of Circular Tubes with Large Side Openings.' *Int. J. Mech. Sci,* Vol. **35** No **3/4**, pp193-108, (1993)

12. N.K. Gupta and S. K. Gupta, 'Effect of Annealing, Size and Cutouts on Axial Collapse Behavior of Circular Tubes.' *Int. J. Mech. Sci*, Vol **35**, No **7**, pp 597-613, (1993)

13. N. Jones, *Structural Impact*, Cambridge University Press, Cambridge, pp. 385-427 (1989)

14. K.R.F. Andrews, G. L. England and E. Ghani, 'Classification of the axial collapse of cylindrical tubes under quasi-static loading.' *Int. J. Mech. Sci.* **25**, pp. 687 - 696 (1983)

15. H. Korneck, 'An Investigation into the Response of Square Box Columns to Axial Loading.' Undergraduate Thesis, University of Cape Town. (1992)

16. C.L. Magee and P.H. Thornton, 'Design Considerations in Energy Absorption by Structural Collapse.' SAE 780434.

17. Q. Meng, S.T.S. Al-Hassani and P. D. Soden, 'Axial crushing of square tubes.' *Int. J. Mech. Sci.* **25**, 747 - 773 (1983)

18. T. Wierzbicki and W. Abramowicz, 'On the Crushing Mechanics of Thin Walled Structures.' *J. Appl. Mech.* **50**, pp. 727 - 734, (1983)

19. T. Wierzbicki and T. Akerstrom, 'Dynamic Crushing of Strain Rate Sensitive Box Columns.' SAE Paper No. 770592.

20. Y. Ohkubo, T. Akamatsu, and K. Shirasawa, 'Mean Crushing Strength of Closed-Hat Section Members.' SAE 740040.

21. W. Johnson, P. D. Soden, and S.T.S. Al-Hassani, 'Inextensional Collapse of Thin-Walled Tubes under Axial Compression.' *J. Strain Anal.*, Vol **12** No. **4**, pp 747 - 773, (1977)

22. E. Haug, F. Arnaudeau, J. Dubois, and A. de Rouvray, 'Static and dynamic finite element analysis of structural crashworthiness in the automotive and aerospace industries.' in *Structural Crashworthiness,* eds N. Jones and T. Wierzbicki (London: Butterworths, 1983)

23. S. Haβ, 'Zur Untersuchungsmethodik axial belasteter Personenkraftfahrzeug-Langstrager mit nichtlinearen Finite-Element-Methoden.' Schriftenreihe Automobiltechnik. (1989)

24. A.G. Pugsley ,' The crumpling of tubular structures under impact conditions. Proc. Symp. *The Use of Aluminium in Railway Rolling Stock*,, Inst. Loco. Engrs., pp. 33-41. The Alumnium developement Association, London (1960), cited by Abramowicz and N. Jones, 'Dynamic axial crushing of circular tubes,' *Int. J. Impact Engng*, Vol **2,** No **3,** pp. 263-281, (1984)

25. T. Wierzbicki and S.U. Bhat, 'A moving hinge solution for axi-symmetric crushing of tubes.' *Int. J. Mech. Sci.* **28**, 135 - 152 (1986)

26. W. Abramowicz, 'The Effective Crushing Distance in Axially Compressed Thin-walled Metal Columns.' *Int. J. Impact Engng.* **1**, pp. 309 -317, (1983)

27. R.J. Hayduk and T. Wierzbicki, 'Extensional Collapse Modes of Structural Members.' *Proc. Symp. Advances and Trends in Structural and Solid Mechanics*, Washington, pp 405 -434, (1982) cited in Abramowicz and N. Jones, 'Dynamic axial crushing of square tubes,' *Int. J. Impact Engng*, Vol **2,** No **2,** pp. 179-208, (1984)

28. W. Abramowicz and T. Wierzbicki, 'Axial Crushing of Multicorner Sheet Metal Columns.' *J. Appl. Mech.* **56**, pp 113 - 120, (1989)

29. R.C. VanKuren and J.E. Scott, 'Energy Absorption of High-Strength Steel Tubes under Impact Crush Conditions.' SAE Paper No. 770213.

30. A.G. Mamalis and W. Johnson, 'The quasi-static crumpling of thin walled circular cylinders and frusta under axial compression.' *Int. J. Mech. Sci.* **25**, 713 - 732 (1983)

31. A.G. Mamalis and W. Johnson, 'The crumpling of steel thin-walled tubes and frusta under axial compression at elevated strain-rates: some experimental results.' *Int. J. Mech. Sci.* **25**, 713 - 732 (1983)

32. G. Belingardi, A. Chiara, and R. Vadori, 'Experimental Evaluation of the Axial Crushing Behavior of Thin Walled Columns of Different Cross-Sections.' *Proc. Conf. Innovation and reliability in automotive design and testing.* Firenze, Italy(1992)

33. G. Belingardi, M. Avalle and A. Chiara, 'Crushing Behavior of Aluminium Circular Tubes.' *Conf. Proc. Structural materials and processes for the transportation industry,* Firenze, Italy (1994)

34. E.J. Hearn,'Mechanics of Materials.'Second Ed. Volume 2, Pergamon Press, pp 457-479. (1985)

35. J.M. Gere, S.P Timoshenko,'Mechanics of Materials.' Second SI Ed. PWS Engineering, Boston (Mass.) (1987)

36. M. Langseth, T. Berstad, O.S. Hopperstad and A.H. Clausen, 'Energy Absorption in Axially Loaded Square Thin-Walled Aluminium Extrusions.' *Structures Under Shock and Impact.* pp401 -410, *Structures under shock and Impact* (1994)

37. D. Hui, 'Design of Beneficial Geometric Imperfections for Elastic Collapse of Thin-walled Box Collumns.' *Int. J. Mech. Sci,* Vol **28**, No **3**, pp 163-172, (1986)

38. K. Durkin, 'An Analytical Method for Predicting the Ultimate Capacity of a Dented Tubular Member.' *Int. J. Mech. Sci,* Vol **33**, pp 449, (1991)

39. S. Li, and S.R. Reid, 'Relationship Between the Elastic Buckling of Square Tubes and Rectangular Plates.' *J. Appl. Mec.*, Vol **57**, pp 969-973, (1990)

40. A. Radford, 'Loading Conditions of Fully Clamped Circular Plates.' Undergraduate Thesis, University of Cape Town. (1992)

BIBLIOGRAPHY

G. Belingardi, A. Chiara, M. Martinotti, R. Vadori, 'Experimental evaluation of the quasi-static collapse of automotive front beams made of glass fibre reinforced plastics.' *II Polish-Italian Seminar*, Torino (Italy) pp 245-252 (1993)

G. Belingardi,and R. Vadori, ' On the role of geometric imperfections in the impact collapse of thin walled spot-welded beam: numerical and experimental results.' *AMD-Vol 169/BED-Vol 25 Crashworthiness and occupant protection in transportation systems*, New Orleans, pp. 115-125 (1993)

N. Jones,'Dynamic elastic and inelastic buckling of shells. Developements in Thin Walled structures (Edited by J. Rhodes and A.C. Walker) Vol 2 pp49-91. Elsevier Applied Science Publishers, Amsterdam (1984)

N. Jones, R.S. Birch,'Dynamic and static axial crushing of axially stiffened cylindrical shells.' *Thin-walled Structures* **9** 29-60 (1990)

D. Kecman, 'Bending collapse of rectangular and square section tubes.' *Int. J. Mech. Sci.* **25**, 623 - 636 (1983)

S.R. Reid, S.L.K. Drew,' Energy Absorbing capacities of braced metal tubes.' *Int. J. Mech. Sci,* Vol **25**, No **9-10**, pp 649 - 667 (1983)

S.R. Reid, 'Plastic deformation mechanisms in axially compressed metal tubes used as impact energy absorbers.' *Int. J. Mech. Sci,* Vol 3**5**, No 12, pp 1035 - 1052 (1993)

Appendix I

As an example of how fast a motor vehicle would be travelling in order for plastic buckling to occur, consider a typical motor vehicle accident in which a vehicle of mass 1 500 kg collides at 50 km/h ($\approx$ 14 ms^{-1}) with a solid wall. The vehicle is assumed to come to rest up against the wall, i.e. an inelastic collision, and all the kinetic energy is dissipated in the crumpling of a number (n) of tubular structures in the front end of the vehicle through a distance Δ.

Kinetic Energy lost by the moving vehicle:

$$KE_l = \frac{1}{2} m v_o^2$$

Energy absorbed by the plastic crumpling of the tubes:

$$E = nP_m \Delta$$

Equating the energies gives:

$$a = \frac{v_o^2}{2\Delta}$$

Since the crushing load is assumed constant, the acceleration is also constant and the instantaneous velocity is:

$$v = v_o + at$$

and the total response time (time to v = 0) is:

$$T = -\frac{v_o}{a}$$

thus substituting in the expression for a gives:

$$T = -\frac{2\Delta}{v_o}$$

If nP_m is such that Δ is 1.5 m, and since the typical velocity of an elastic stress wave travelling in mild steel is approximately 5150 ms^{-1}. This means that it takes approximately 0.3 ms to travel down a 1.5m mild steel tube. In order for plastic buckling to occur instead of progressive buckling, the pulse must be in the order of .0.3 ms and thus the impact velocity of the car about 10 000ms^{-1}. This is clearly unreasonable. The mass of the vehicle is also much greater than the mass of the energy absorbing tubes.

Appendix II

Measurement of Applied Impulse

The impulse is given by

$$I = M\dot{x}_o$$

where M is the total mass of the pendulum with all its attachments and $\dot{x}_o$ is the initial velocity of the pendulum.

The equation of motion for the pendulum is assumed to be given by:

$$M\frac{d^2x}{dt^2} + C\frac{dx}{dt} + \frac{M}{R}gx = 0$$

where x is the horizontal displacement, C is the damping coefficient, and R is the radius of the pendulum motion.

if $\beta = \frac{C}{2M}$ and $\omega_d = \frac{2\pi}{T}$ and T is the period of the pendulum motion, then the solution to equation 2.1 is

$$x = e^{-\beta t}\frac{\dot{x}_o}{\omega_d}\sin(\omega_d t)$$

where β is the damping constant and ω_d is the circular frequency.

If x_1 is the horizontal displacement at time $t = \frac{T}{4}$ and

$-x_2$ is the horizontal displacement at time $t = \frac{3T}{4}$ then

from equation 3.2, the first horizontal oscillation x_1 is given by

$$x_1 = e^{-\beta T/4}\dot{x}_o\frac{T}{2\pi}\sin\frac{2\pi}{T}\frac{T}{4}$$

which becomes

$$x_1 = e^{-\beta T/4} \dot{x}_o \frac{T}{2\pi}$$

similarly

$$-x_2 = e^{-3\beta T/4} \dot{x}_o \frac{T}{2\pi} \sin\frac{2\pi}{T}\frac{3T}{4}$$

which becomes

$$x_2 = e^{-3\beta T/4} \dot{x}_o \frac{T}{2\pi}$$

now

$$\frac{x_1}{x_2} = e^{\frac{1}{2}\beta T}$$

therefore

$$\beta = \frac{2}{T} \ln\frac{x_1}{x_2}$$

and

$$\dot{x}_o = x_1 \frac{2\pi}{T} e^{\beta T/4}$$

The period T can be measured and β can be found from a number of swings of the pendulum. In order to find x_1 and x_2 the geomerty of the pendulum swing is required.

APPENDIX III

Tensile Test Data

w : width of parallel section
t : thickness of parallel section
lo : origional gauge length
lu : gauge length after failure

strain rate : (crosshead speed)/(lo)
yield' : dynamic yield strength
UTS' : dynamic ultimate tensile strengt
% elongation : (lo-lu)/lo

static yield : static yield stress calculated from the Cowper-Symonds eqn
static UTS : static ultimate tensile stress calculated from the Cowper-Symonds eqn
D, q : Cowper Symonds constants

stress: average static yield (/UTS
pmax : predicted ultimate buckling load of origiona undeformed tube (eqn

D :									40.4 [13]		802 [4]		6844 [4]	
q :									5		3.585		3.91	
test	w	t	lo	lu	strain rate /s	elongatio	yield' MPa	UTS' MPa	static yield MPa	static UTS MPa	static yield MPa	static UTS MPa	static yield MPa	static UTS MPa
A1	12.52	1.24	50.2	67.5	8.4E-04	34%	323	384	289	344	316	376	317	377
A2	12.46	1.22	50.3	68.4	8.4E-03	36%	322	377	272	319	309	363	312	366
A3	12.5	1.24	50.3	66.6	8.4E-02	32%	380	398	294	309	353	370	360	377
stress									285	324	326	369	330	374
pmax									65031	73861	74323	84243	75219	85225
B0	12.5	1.28	50.3	66.9	8.4E-02	33%								
B1	12.5	1.26	50.4	67.6	8.4E-04	34%	319	380	286	341	312	372	314	374
B2	12.48	1.26	50.3	67.7	1.7E-03	35%	305	367	270	324	298	357	299	359
B3	12.48	1.28	50.2	66.6	8.4E-03	33%	322	378	272	319	309	363	312	366
B4	12.56	1.28	50.3	66.2	4.2E-02	32%	332	374	265	298	312	352	317	357
B5	12.5	1.3	50.4	66.4	8.4E-02	32%	361	379	280	294	335	352	342	359
stress									274	315	313	359	317	363
pmax									62602	71870	71465	81913	72299	82844

									D :	40.4 [13]		802 [4]		6844 [4]	
									q :	5		3.585		3.91	
test	w	t	lo	lu	strain rate /s	elongatio	yield' MPa	UTS' MPa	static yield MPa	static UTS MPa	static yield MPa	static UTS MPa	static yield MPa	static UTS MPa
C1	12.54	1.24	50.4	66.8	8.4E-04	33%	312	363	279	326	305	356	307	357
C2	12.46	1.24	49.5	64.5	1.7E-03	30%	332	387	293	342	324	378	326	380
C3	12.16	1.24	50.5		8.4E-03		307	376	259	318	295	362	298	365
C4	12.5	1.24	49.6	64.7	4.3E-02	31%	358	398	286	318	337	374	342	381
C5	12.46	1.26	49.5	63.3	8.6E-02	28%	380	398	294	308	352	369	360	377
stress									282	322	322	368	326	372
pmax									64374	73488	73550	83847	74421	84816
D1	12.58	1.98	49.8	64.1	8.5E-04	29%	288	373	258	334	281	365	283	367
D2	12.54	2	49.9		1.7E-03		275	347	243	306	268	338	269	340
D3	12.52	2	50.1	67.4	8.4E-03	35%	262	347	221	293	252	334	254	337
D4	12.54	1.98	49.7	66.0	4.3E-02	33%	285	365	227	291	268	343	272	348
D5	12.62	1.98	50.1		8.4E-04		313	380	281	341	307	372	308	374
D6	12.6	1.98	50.1	64.7	8.5E-02	29%	301	367	233	284	280	341	285	348
stress									244	308	276	349	279	352
pmax									180877	228694	204636	258706	206723	261335
E1	12.46	2	49.4	68.7	8.6E-04	39%	292	352	261	315	286	344	287	346
E2	11.96	1.98	50.4	67.8	1.7E-03	34%	280	350	247	309	273	341	274	343
E3	12.6	2	49.9	64.2	8.5E-03	29%	290	362	245	306	279	348	282	351
E4	12	1.98	50.1	66.2	4.2E-02	32%	298	365	237	291	280	343	284	349
E5	12.66	1.98	49.9	66.6	8.5E-02	34%	315	373	244	289	292	346	298	353
stress									247	302	282	344	285	348
pmax									183261	223998	209112	255509	211534	258450
Specimens cut from tube seam														
Aw	12.42	1.26	50.0	59.0	8.5E-03	18%	426	477	360	403	410	458	414	463
Bw	12.56	1.28	50.6	58.7	8.4E-03	16%	431	471	364	398	414	453	418	457
Cw	12.42	1.24	50.0	58.7	8.5E-03	17%	448	497	378	420	430	477	434	482
Dw	12.5	2	50.0	57.2	8.5E-03	15%	402	479	340	404	386	460	390	464
Ew	12.06	1.98	50.3	57.7	8.4E-03	15%	382	436	323	368	367	419	370	423

APPENDIX IV

Explosive callibration

m : Explosive mass
l : explosive length
w : explosive width
h : explosive height
I : Explosive Impulse calculated as shown in appendix II

Cd : depth of deformation at tube centre
Ed : depth of deformation at tube corners
Cl : length of deformation at tube centre
El : length of deformation at tube corners

STRIP EXPLOSIVE CALIBRATION

TEST NO.	m g	l mm	w mm	h mm	I Ns	Cd mm	Ed mm	Cl mm	El mm
13049405	6.5	55.0	5.0	15.3	5.90	18	6	159	134.5
21049404	6.5	55.0	5.0	15.3	5.90	15	3.5	167	111.5
21049403	6.5	55.0	6.3	12.1	6.83	24	9.5	146	126.5
13049406	6.5	55.0	6.3	12.1	6.78	22.5	9	162	140.75
21049402	6.5	55.0	8.0	9.6	7.19	28	11	145	128.5
13049407	6.5	55.0	8.3	9.2	6.84	28	11.5	145	132.5
20049409	6.5	55.0	8.3	9.2	7.34	27	10.25	147	129.5
21049401	6.5	55.0	8.7	8.8	7.31	29	11.5	143	132
20049408	6.5	55.0	9.1	8.4	7.32	32	13.5	144	127.25
13049408	6.5	55.0	9.5	8.1	7.53	30	13	144	121
20049405	6.5	55.0	9.1	8.4	7.48	-	20	105	95.5
20049407	6.5	55.0	9.5	8.1	7.29	-	25.5	103	92.5
20049403	6.5	55.0	9.5	8.1	7.61	-	18.75	108.5	98.5
20049404	6.5	55.0	9.5	8.1	7.37	-	24	94	89
20049402	6.5	55.0	10.0	7.6	7.58	-	18	113	100
20049406	6.5	55.0	10.0	7.6	7.62	-	23	100.5	90.5
20049401	6.5	55.0	12.0	6.4		-	20.25	94.5	91
21049405	6.5	55.0	13.9	5.5	7.58	-	27	94	89.5
13049409	6.5	55.0	14.4	5.3	7.73	-	27	84	73
25059411	5.75	55.0	12.0	5.6	7.29	-	25	93	85.5
25059412	5.75	55.0	10.0	6.8	7.19	-	13	125	109.25
25059413	5.75	55.0	8.0	8.5	6.61	27	10.5	144	125.5
23059408	5.0	55.0	5.0	11.8	5.05	16.3	4.7	143	114
23059407	5.0	55.0	8.3	7.1	5.78	22.2	9.4	130	118.5
23059401	5.0	55.0	9.5	6.2	6.05	24	9.3	133	121.5
23059402	5.0	55.0	10.8	5.4	6.46	26.2	10.95	134	125
25059401	5.0	55.0	12.0	4.9	7.39	29	12	134	119
23059403	5.0	55.0	13.0	4.5	6.61	30	12.1	130	123
23059406	5.0	55.0	13.0	4.5	6.61	-	17.05	109	102
23059405	5.0	55.0	14.0	4.2	6.80	-	15.9	113	102.5
23059404	5.0	55.0	15.0	3.9	6.75	-	22.1	87	81.5
25059404	5.0	48.0	5.0	13.5	5.44	16	4.7	150	105.5
23059411	5.0	48.0	8.0	8.4	5.97	23.3	9.3	134	116
23059412	5.0	48.0	9.1	7.4	5.95	25.2	9.9	130	111.5
25059403	5.0	48.0	10.0	6.7	6.14	22	11.3	131	112
23059413	5.0	48.0	10.8	6.2	6.39	-	20	101	92.5
25059402	5.0	48.0	12.0	5.6		-	24.5	93	74
25059409	5.0	44.0	5.0	14.7	5.44	20	6.2	144	119.5
25059408	5.0	44.0	8.0	9.2	6.07	26.4	9.9	145	134

STRIP EXPLOSIVE CALIBRATION

TEST NO.	m g	l mm	w mm	h mm	I Ns	Cd mm	Ed mm	Cl mm	El mm
25059410	5.0	44.0	8.3	8.9	5.73	26	9	144	119.5
25059407	5.0	44.0	9.1	8.1	6.48	-	22.4	95	87
25059406	5.0	44.0	10.0	7.4	6.27	-	17.4	110	99
25059405	5.0	44.0	12.0	6.1	6.66	-	25	95	89.5
13059401	3.5	55.0	3.2	12.9	3.50	8.4	0.7	138	90.5
13049402	3.5	55.0	5.0	8.2	3.61	11	2.75	125	102
13059402	3.5	55.0	6.3	6.5	4.08	13	3.7	121	96.5
13059404	3.5	55.0	8.0	5.1	4.61	17	5.75	120	105
13059405	3.5	55.0	10.0	4.1	4.76	17	7.5	120	109.5

Mexp	Mass of Explosive (incl leader)	Edave	Ave depth of corner dent
Dexp	Diameter of explosive	Have	Approx hole diameter
CLave	Length of dent	Hl	Hole length
		Hw	Hole width

ROUND EXPLOSIVE CALIBRATION

TEST NO.	Mexp g	Dexp mm	Edave mm	Have mm	Hl mm	Hw mm	CLave mm
BA1	6	25	2.2	18.5	18	19	185
BA2	8	25	2	22.5	21	24	205
BA3	10	3.05		39.5	35.5	43.5	190
CA1	12	48	7.1	42.5	50	35	190
CA2	9.5	48	6.55		44		215
CA3	9	48	5.8				230
CA4	9.5	48	7.65	41	47	35	215
CA5	14	48	9.85	51.5	53	50	210
DA1	6.5	40	3.45				220
DA2	9	40	4.2		29		210
DA3	8	40	3.85	34.25	36	32.5	210
DA4	10.5	40	4.8	42	42	42	220
EA1	11	52	8.25	45.25	54	36.5	
EA2	14	52	11.25	57	63	51	
DB0		40	0	0			
DB1	8	40	3.5	30.375	32.5	28.25	232.5
DB2	10.5	40	4.25	32.5	32	33	215
DB3	13	40	10.875	64.75	63.75	65.75	208.5
DB4	10.5	40	3	36.75	42	31.5	200
DB5	9	40	3.75	34.75	35.5	34	197.5
DB6	12.5	40	5	51.5	53	50	260
DB7	8.5	40	4.125	33.75	36.5	31	235
EB0							
EB1	8	25	1.5	20.75	20.0	21.5	217.5
EB2	8	40	4.4	30.875	33.0	28.8	210
EB3	10.5	48	6.6	41.5	47.3	35.8	199.5
EB4	12	48	6.5	42.125	48.3	36.0	210
EB5	11	52	9.0	44.875	53.8	36.0	215
EB6	12	52	7.1	45	51.5	38.5	227
EB7	12	55	15.9	47.625	60.3	35.0	216.5

APPENDIX V

Quasi-static tests of mechanically deformed specimens

tube : specimen number
ϕ : hole diameter
Ed : depth of corner dent
length : specimen length
mode : as defined in section 4.3.2
Indenter ϕ : diameter of cylinderical indenter

Pmean : (area under the load-displacement curve) / (total crushed distance)

Tube	ϕ mm	Ed mm	Length mm	Pult kN	Phigh kN	Pmean kN	Mode
A1	0	0	300	74	33	22	sp
A2	16	0	300	69	30	23	sspi
A3	22	0	300	62	28	21	sspi
A4	25	0	300	51	31	21	ebi
A5	32	0	300	52	25	22	t
A6	38	0	300	45	18	15	t
G1	0	1.3	250	52	22	21	sspii - ebii
G2	0	3.75	250	45	27	20	sspii - ebii
G3	0	6	250	42	30	20	sspii - ebii
G4	0	0	250	75	35	19	sp
G5	0	6.5	250	41	30	20	sspii - ebii
G6	0	4	250	45	26	21	sspii - ebii
G7	0	1.5	250	53	30	16	sspii - ebii
G8	16	0	250	72	-	23	sspi
G9	25	6.3	250	36	26	20	sspii
G10	25.7	4	250	37	28	20	sp
G11	25.7	1.5	250	44	33	24	sspi
G12	32	5.9	250	33	34	17	sspii
G13	32.5	4	250	34	34	18	sp
G14	32	1.2	250	41	41	-	sspi
G15	16.4	4	250	40	40	-	sspii
G16	38.4	4	250	31	31	-	sspi
G18	25	0	250	57	30	19	sspi

Tube	Indenter ϕ	Ed mm	Length mm	Pult kN	Phigh kN	Mode
AA0	0	0	300	78	32	sp
AA1	2	5	300	34	34	sp
AA2	2	8.8	300	33		sspii
AA3	2	11.6	300	34		sspii
AB1	30	2.8	300	40	34	sp
AB2	30	5.4	300	31	34	sp
AB3	30	7.6	300	31	28	sspii
AB4	30	8.7	300	33		sspii
AB5	30	11.3	300	34		sspii
AC1	50	2.8	300	42	31	sp
AC2	50	6.1	300	32	31	sp
AC3	50	8.8	300	34	31	sspii
AC4	50	12	300	36		ebii

APPENDIX VI

Quasi-static tests of explosively deformed specimens

tube : specimen number
length : specimen length
dent depth : average depth of corner dents

Pmean : (area under the load-displacement curve) / (total crushed distance)

tube	length mm	hole width mm	hole lengt mm	dent depth mm	Pult kN	Pmean kN	Phigh kN
EB0	527	0	0	0	189.5	50.0	97.5
EB1	526	22	20	1.5	142.5	-	-
EB2	527	29	33	4.4	136.5	-	-
EB3	278	36	47	6.6	130.3	-	-
EB4	528	36	48	6.5	125.5	42.8	80.0
EB5	528	36	54	9.0	121.8	50.7	75.0
EB6	527	39	52	7.1	124.3	47.6	67.5
EB7	524	35	60	15.9	105.5	47.1	70.0
DB0	294	0	0	0.0	173.5	-	109.5
DB1	295	28	33	3.5	141.3	-	111.3
DB2	296	33	32	4.3	133.3	-	-
DB3	295	66	64	10.9	97.5	-	-
DB4	295	32	42	3.0	134.3	-	-
DB5	299	34	36	3.8	134.3	-	-
DB6	294	50	53	5.0	130.5	-	-
DB7	299	31	37	4.1	135.5	-	-

Appendix VII

Example of Data

Figure vii.a shows three force deflection curves superimposed onto each other. The curves were generated by the Instron tester.

Curve G4 shows the collapse of an undeformed tube.

Curve A4 had two 25 mm diameter hole drilled opposite one another prior to collapse.

Curve G6 was pre dented to 4 mm at the corners prior to collapse.

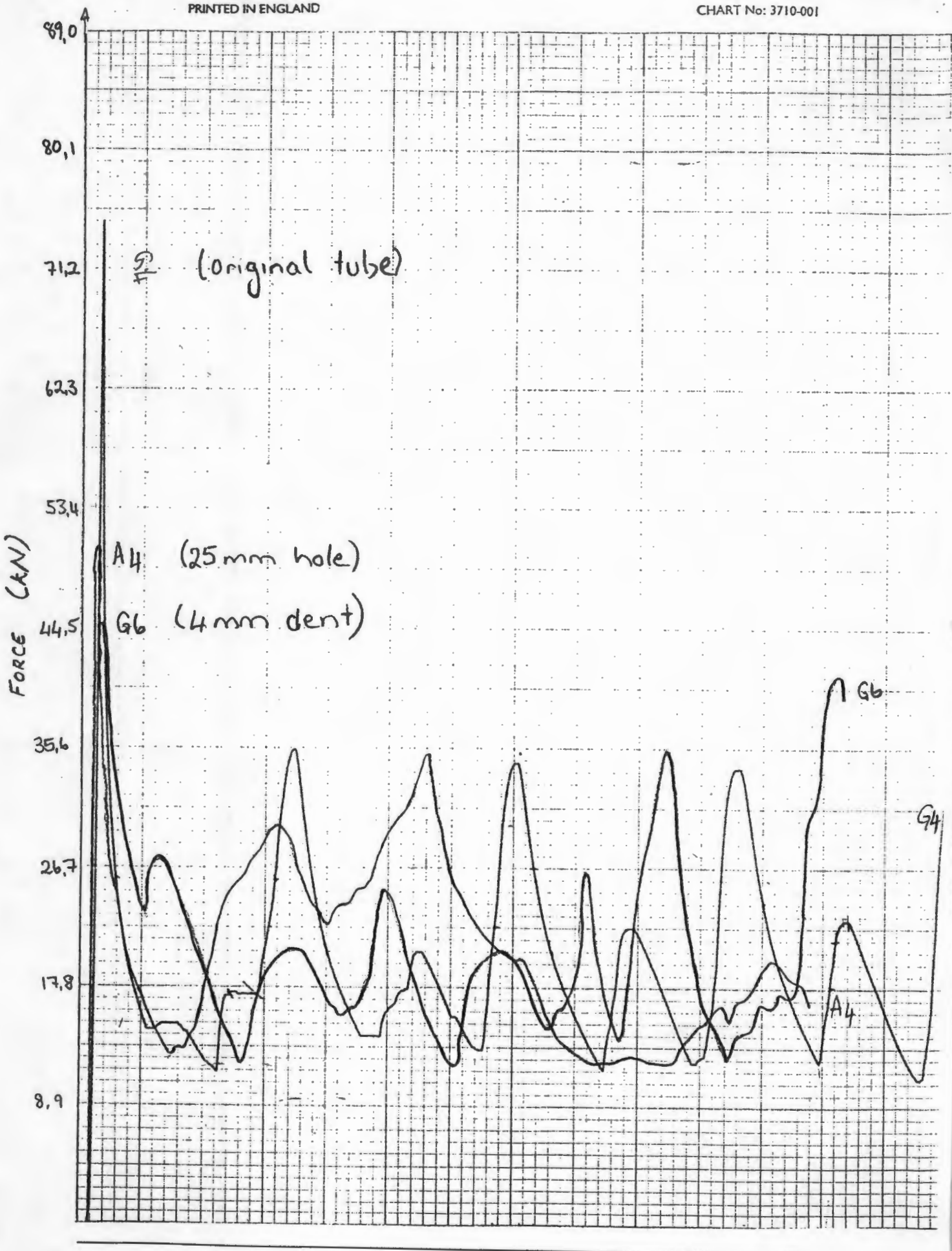
89,0
80,1
71,2
62,3
53,4
44,5
35,6
26,7
17,8
8,9
FORCE (kN)
S1 (original tube)
A4 (25mm hole)
G6 (4mm dent)
G6
G4
A4